CMORE, June 2010
Roman Stocker
MIT

2. Motility and chemotaxis, in general and in the Ocean

- Why and how to swim?
  - Rotating a corkscrew, cracking a whip or coordinating many hairs
- The costs of swimming: a Datsun in Saudi Arabia?
- *E. coli*'s run-and-tumble swimming
- Diffusion of a bacterial population
- Chemotaxis
  - How it works
  - Examples of taxis
- **Recent work on motility and chemotaxis in the Ocean**

Counterintuitive fluid mechanics

(2) Reversibility at low Re

http://web.mit.edu/fluids/www/Shapiro/ncfmf.html

The scallop theorem!

Costs and benefits of swimming for microbes

Why swim?

Find food (encounter it more often (blindly), or actively exploit gradients)
Find mates (in the same manner)
Minimize death by predation (handling, *not* encounter)

Why not?

Energy cost
Signal to predator (you're 'moving water')
Higher encounter rate with predators and viruses
It's difficult to swim if you are small: Brownian reorientation

How to swim? → need to circumvent the scallop theorem!

1) Rotating a rigid, helical flagellum (bacteria)
2) Waving a flexible flagellum (eukaryotes, e.g. sperm, phytoplankton)

→ Both are non-reversible motions and give propulsion

Three types of swimming appendages

Lighthill,1976

Bacterial flagella

e.g. *E. coli*

Cilia e.g. Paramecium

Eukaryotic flagella

e.g. spermatozoa

The eukaryotic flagellum

Flagellum is **flexible:**
→ cell propagates waves down the flagellum
→ from the base to the tip (mostly), like a whip

Waves can be
→ planar (2D)
→ helical (3D)

Powered by dynein molecular motors distributed along the length and circumference of the flagellum, driven by ATP

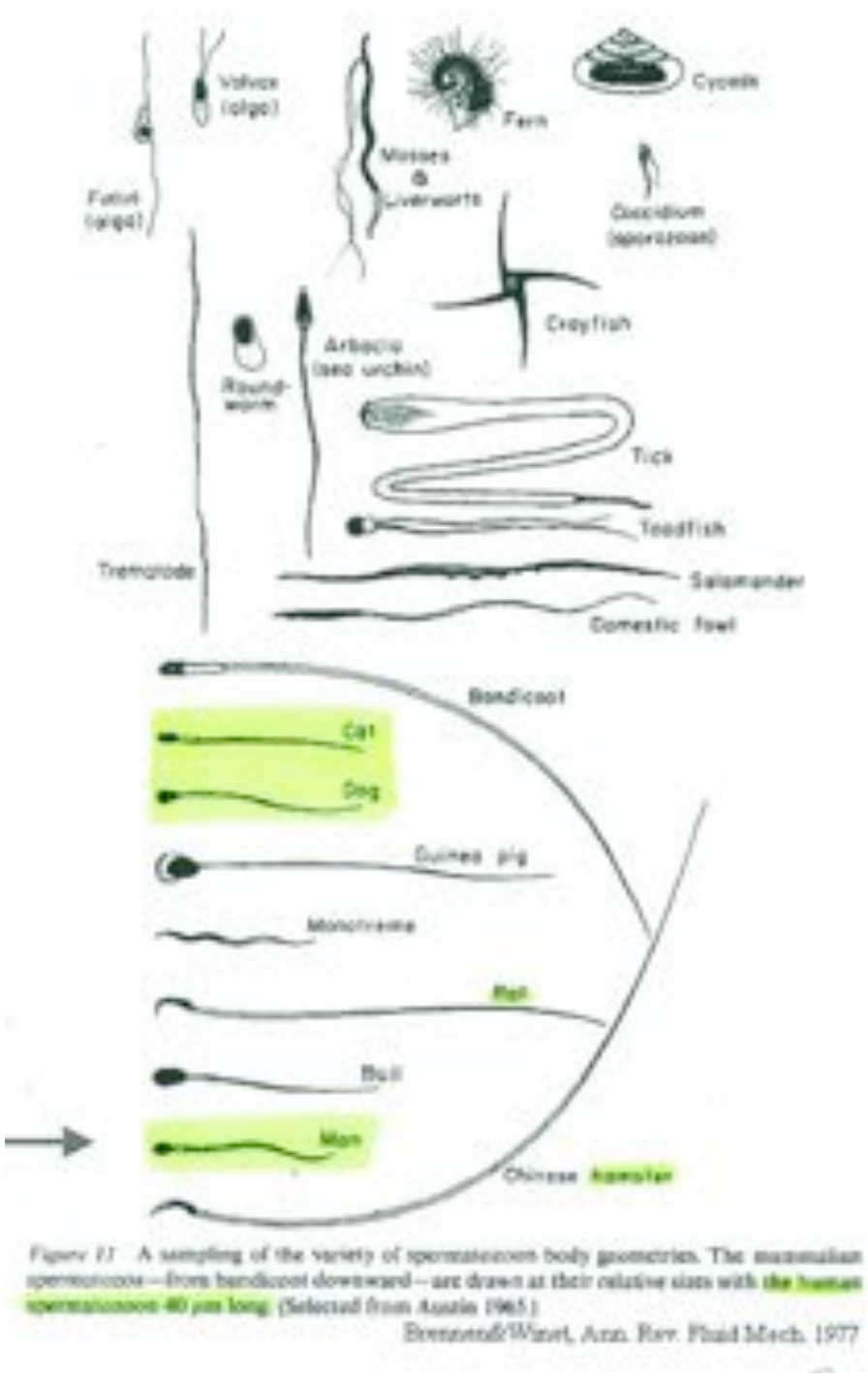

Eukaryotic flagella: phytoplankton

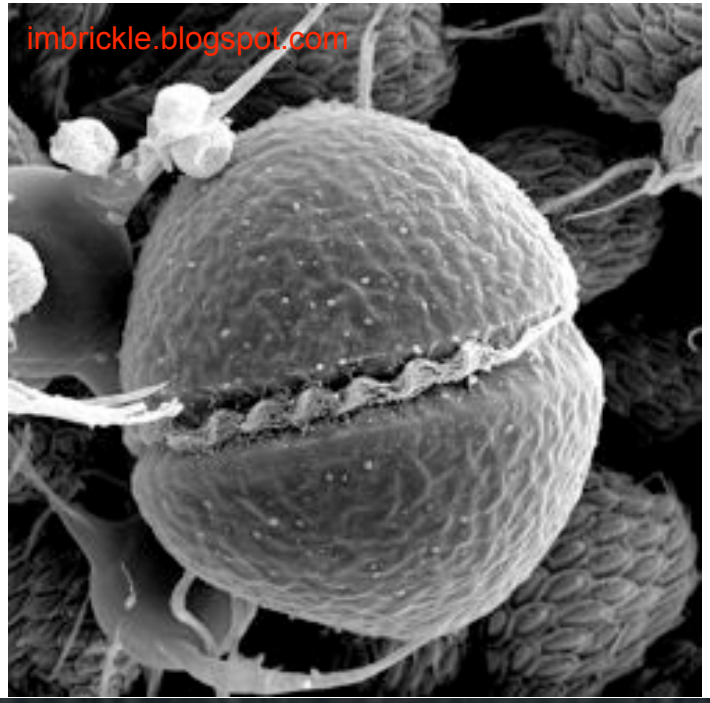

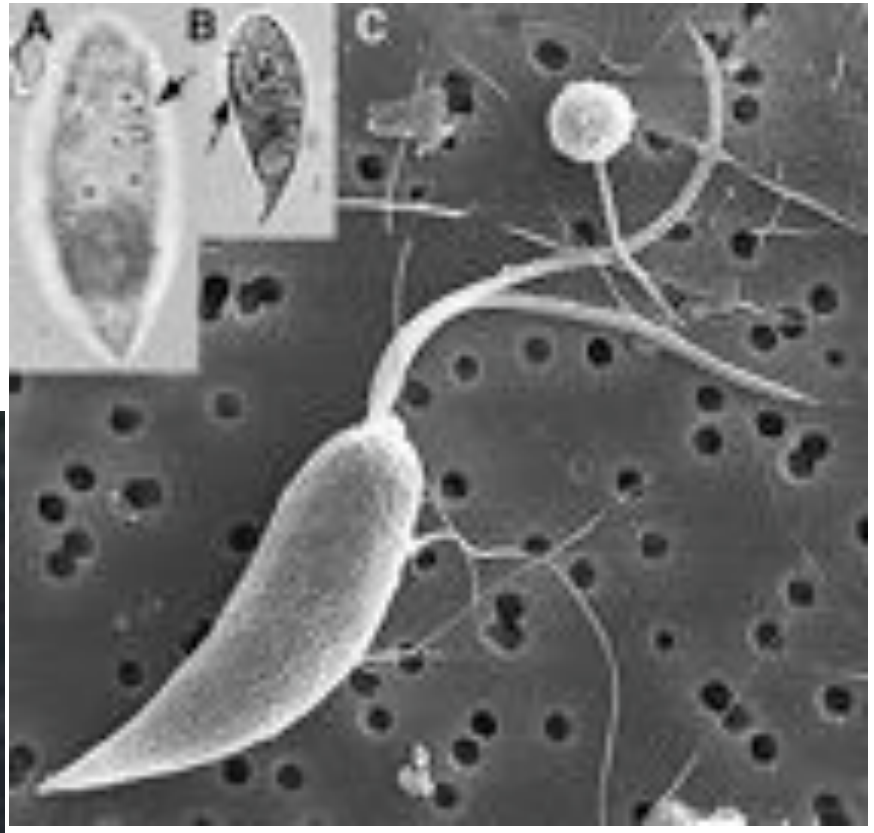

Leucocryptos marina, a marine dinoflagellate (Butcher 1967)

Structure of the eukaryotic flagellum: the axoneme

- Protein: tubulin
- Diameter of the flagellum: 200 nm
- 9+2 structure
- Bending of flagellum: due to sliding between pairs of outer microtubules

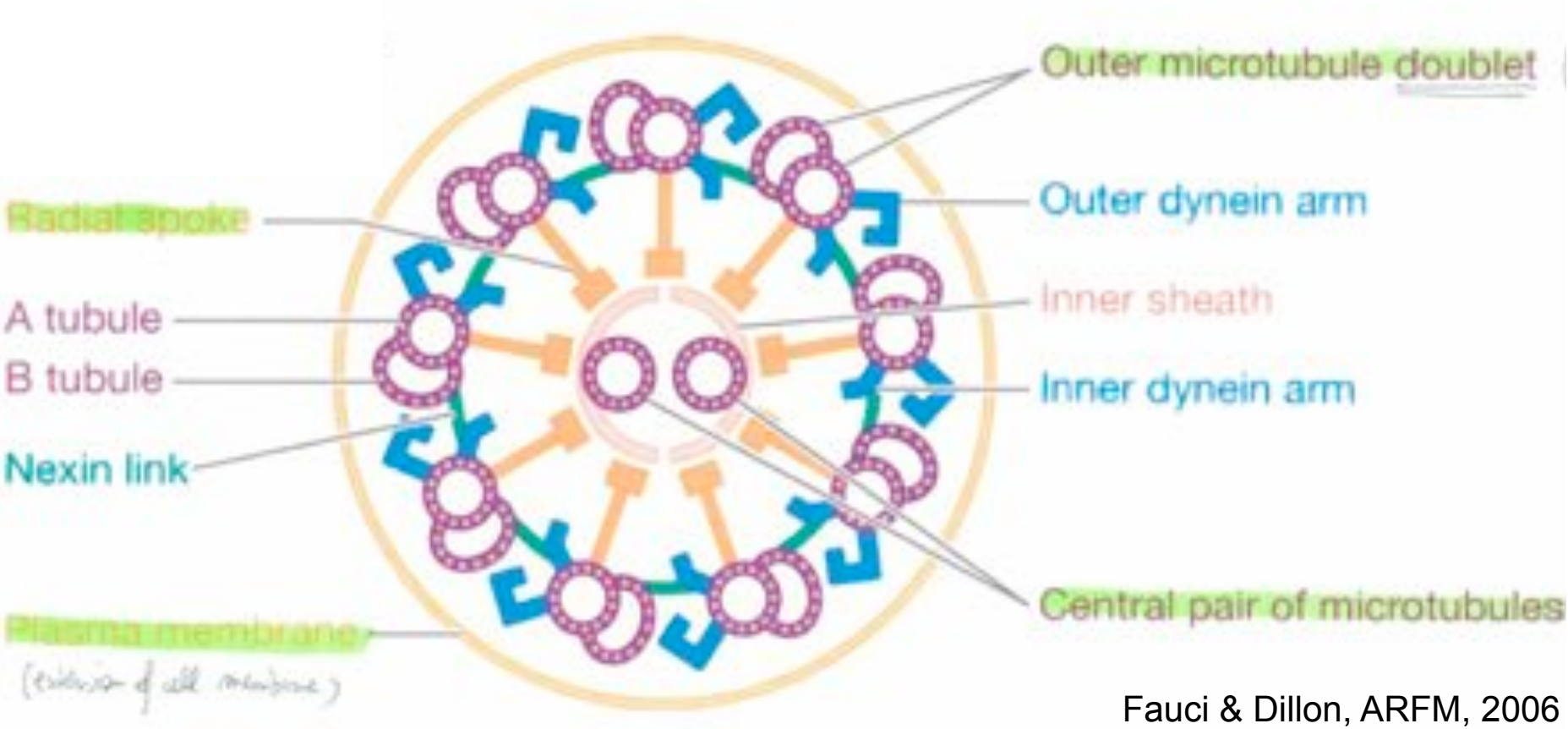

Fauci & Dillon, ARFM, 2006

The prokaryotic flagellum

- Helical and rigid: pitch ~ 2 μm, diameter ~ 20 nm
- Helical protein: flagellin
- Single motor at the base of each flagellum

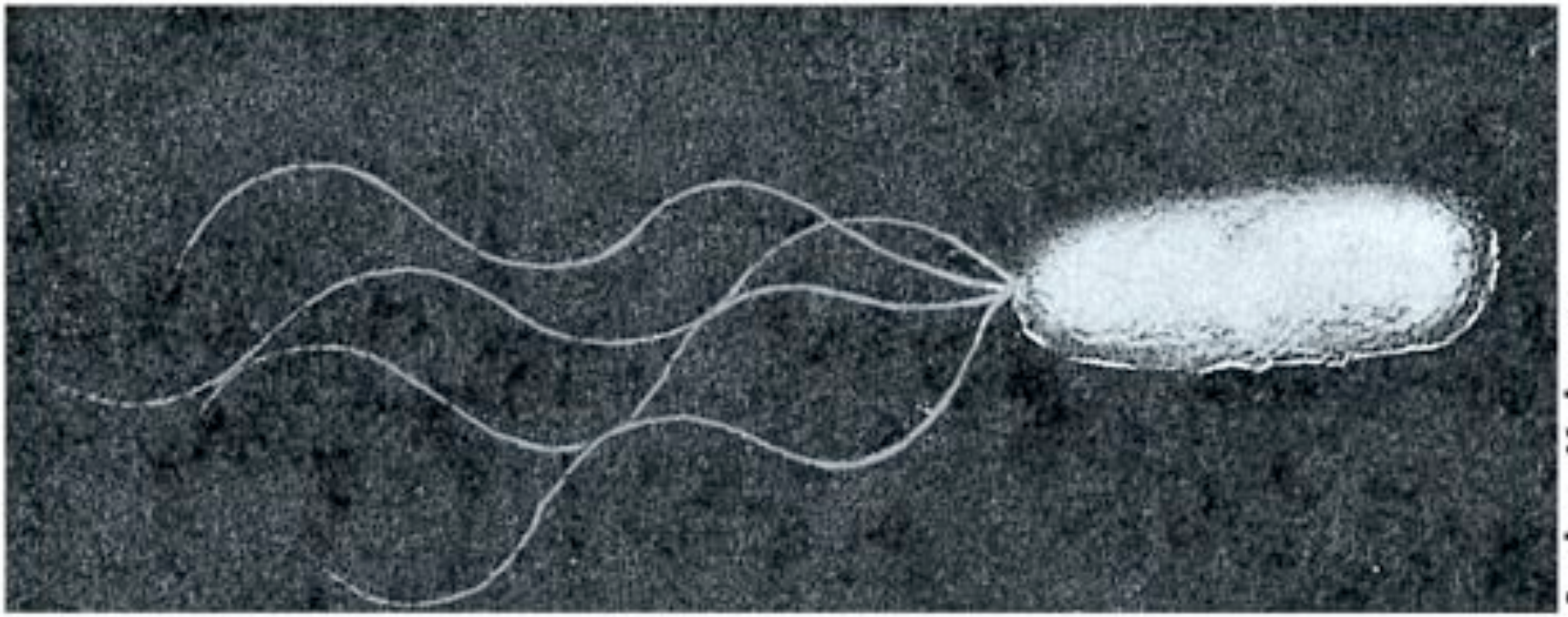

Figure 12-17b Brock Biology of Microorganisms 11/e

Multiple polar flagella

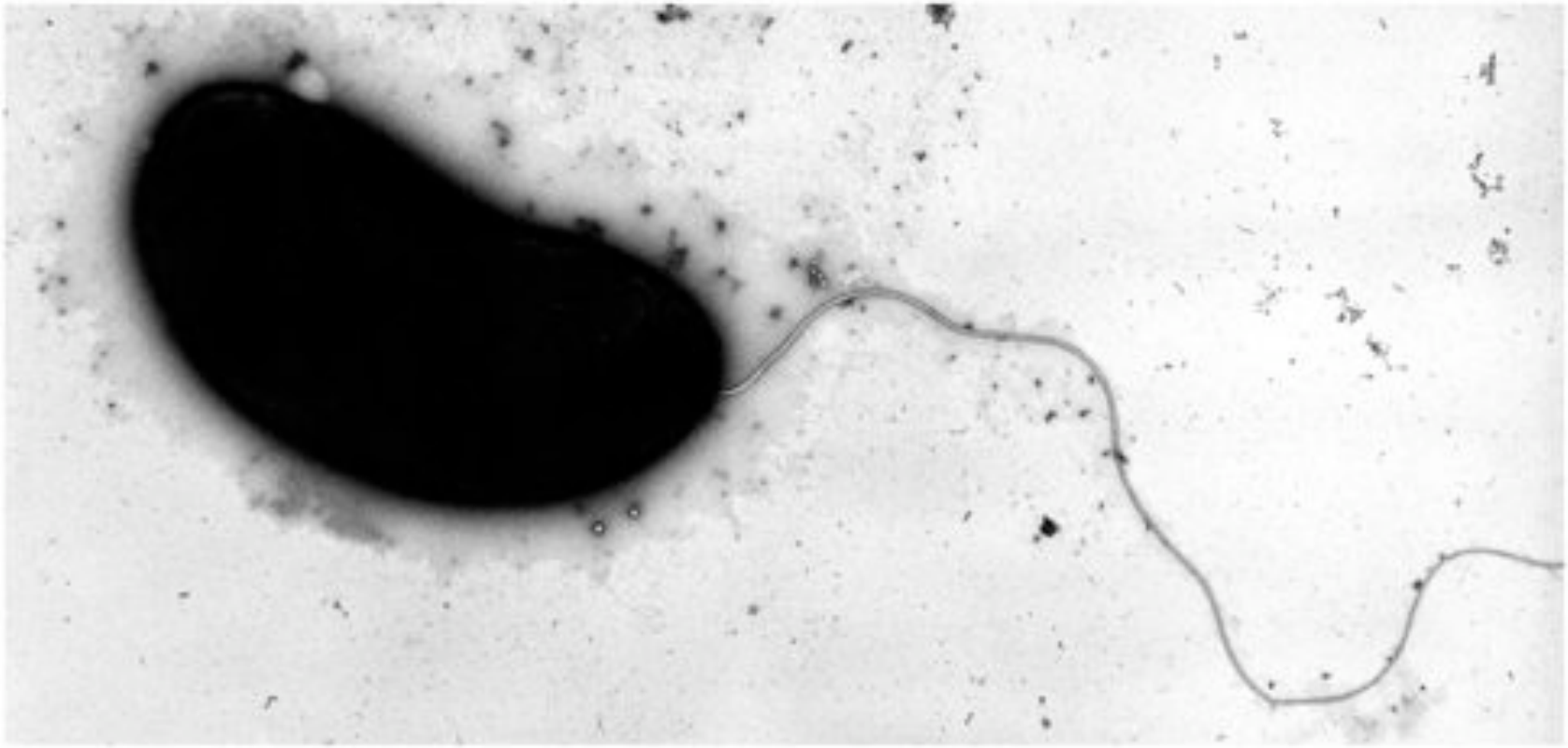

Figure 4-54a Brock Biology of Microorganisms 11/e

One polar flagellum (monotrichous)

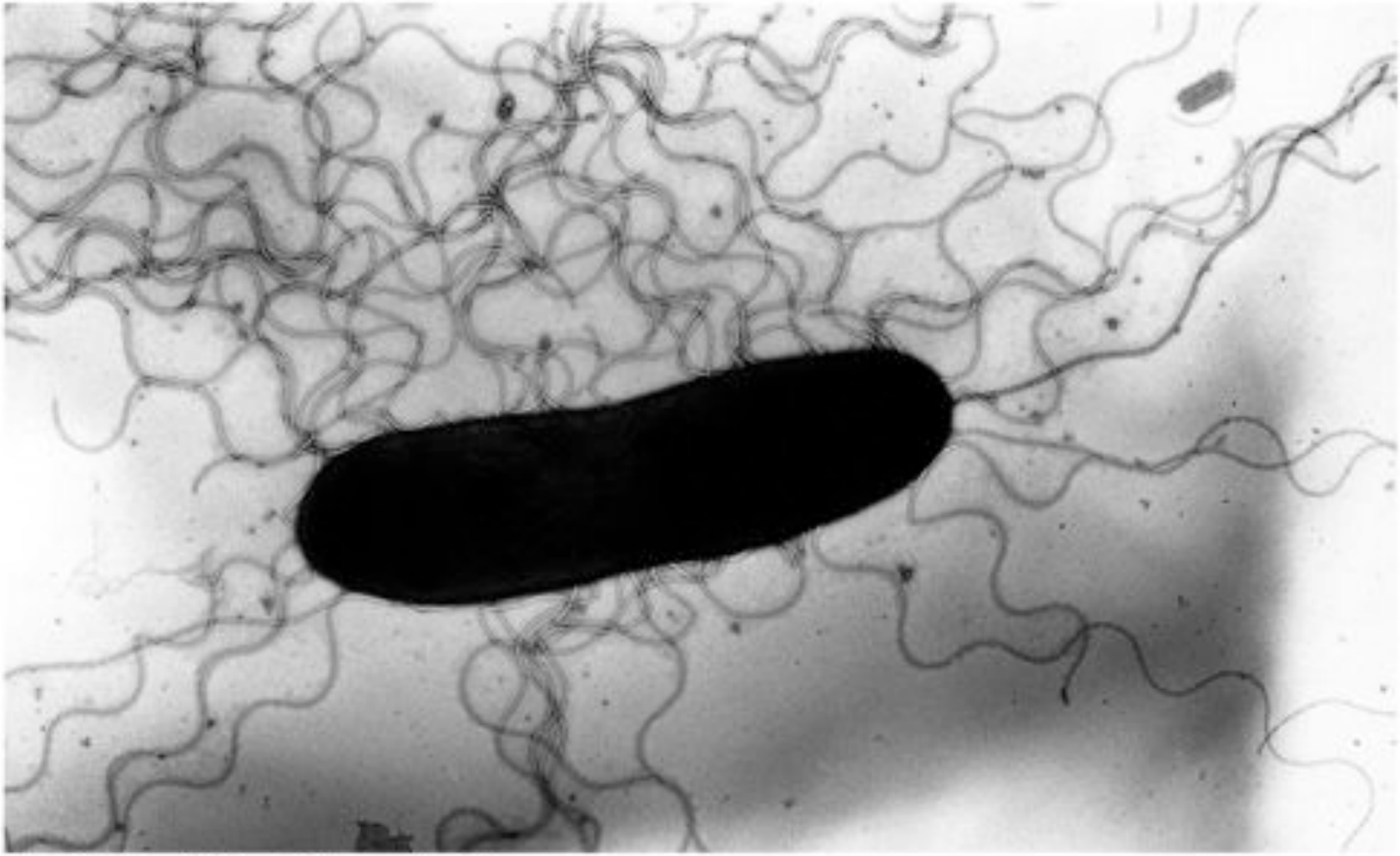

Carl E. Bauer

Figure 4-54b Brock Biology of Microorganisms 11/e

Many flagella, all over the body (peritrichous)

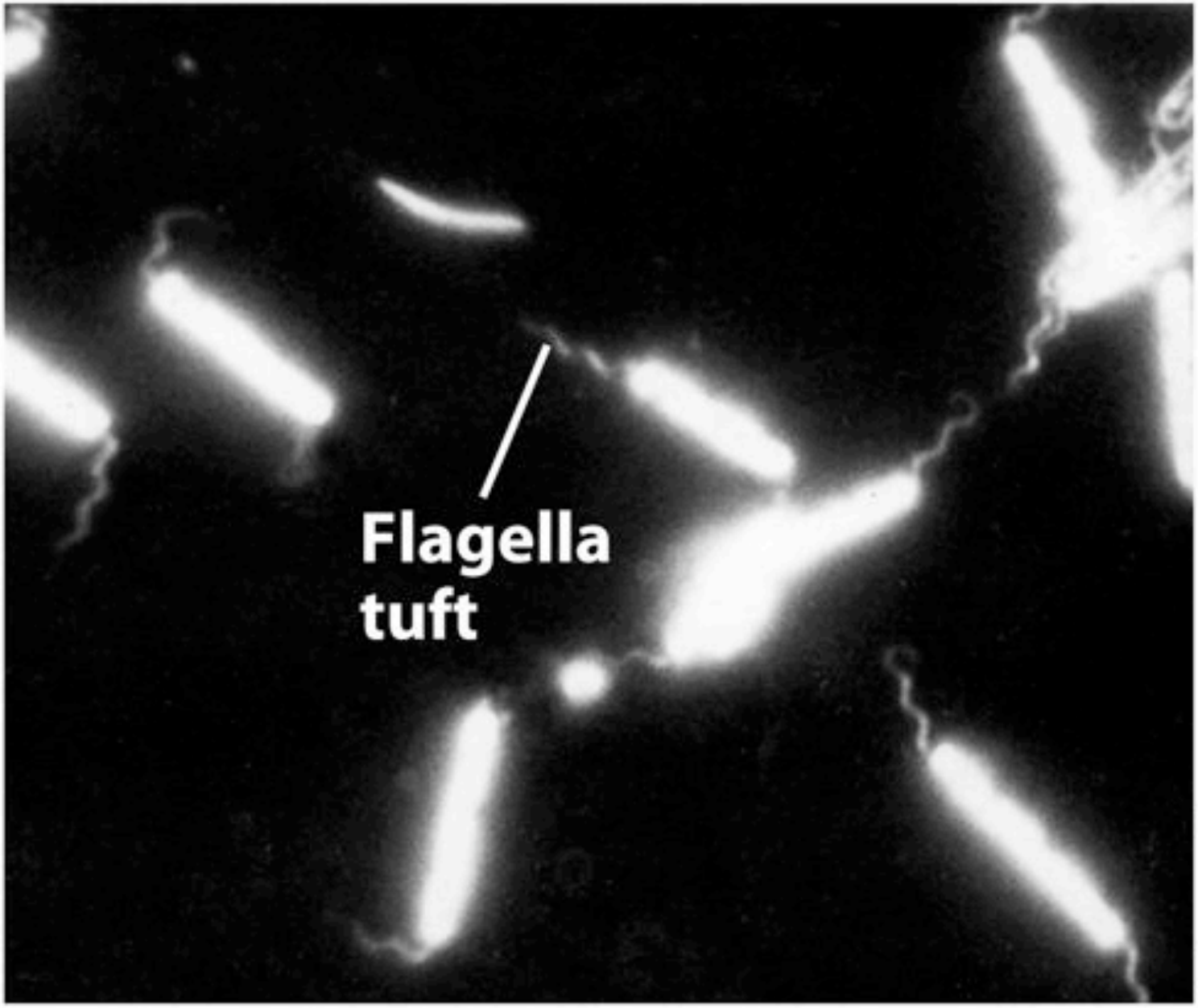

Figure 4-55a Brock Biology of Microorganisms 11/e

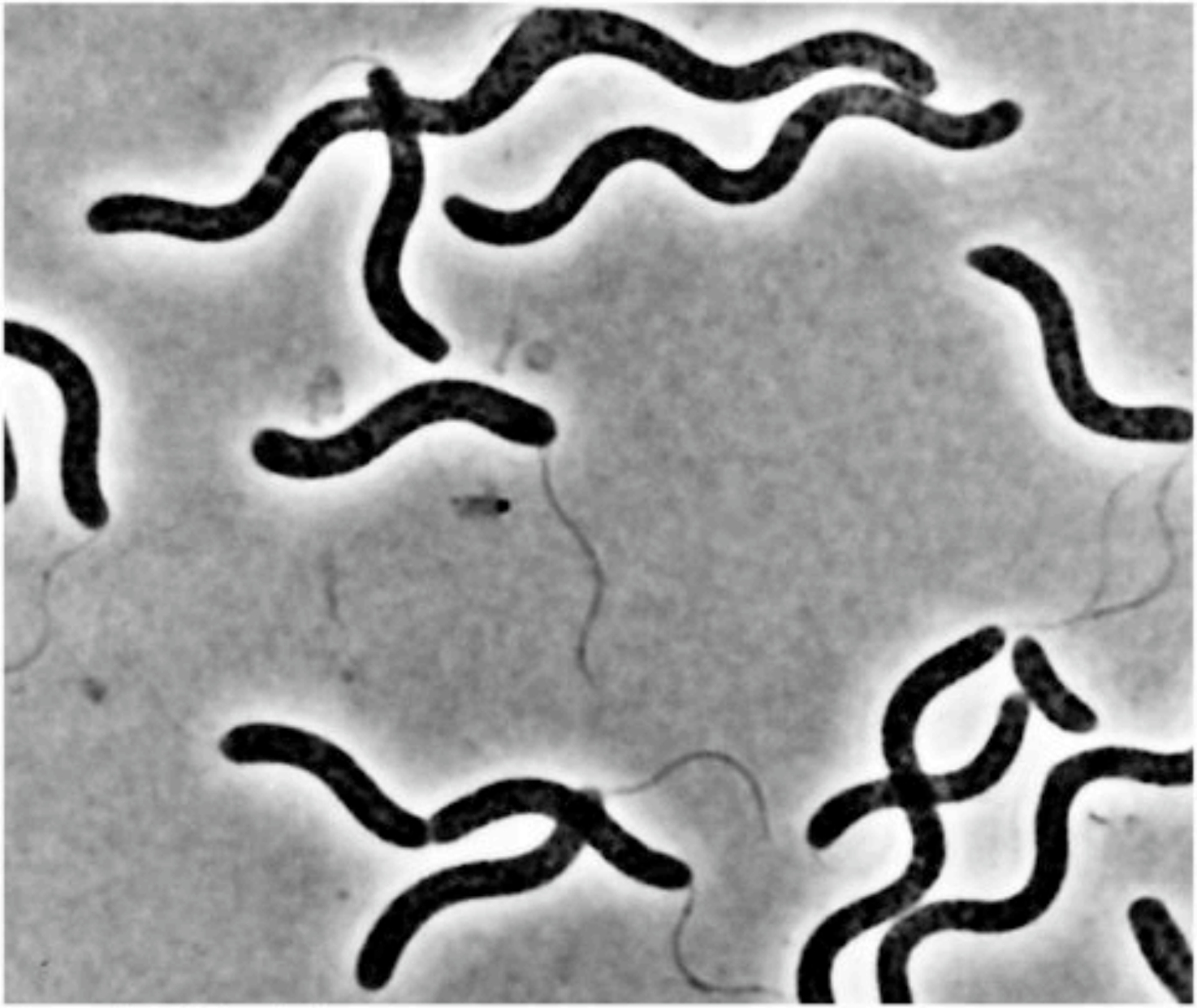

Norbert Pfennig

Figure 4-55b Brock Biology of Microorganisms 11/e

Rhodospirillum photometricum

The molecular motor

Hook-basal body complex

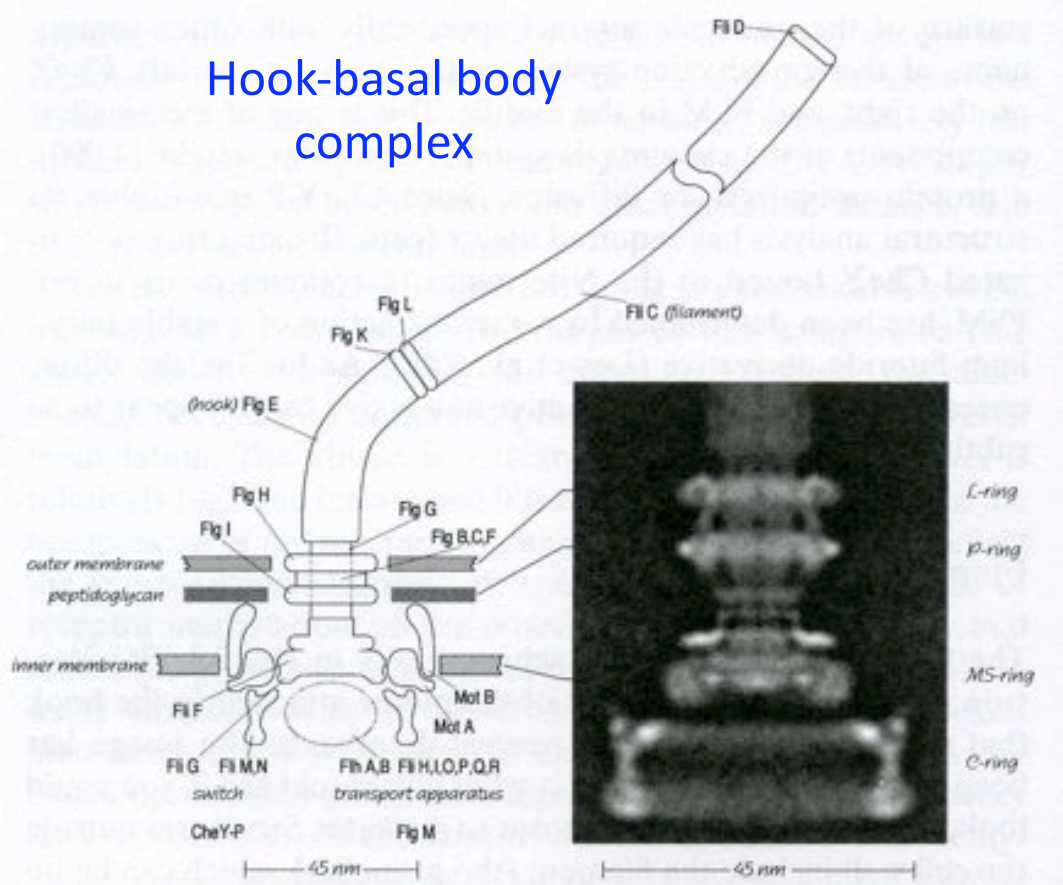

FIGURE 9.3. A schematic diagram of the flagellar rotary motor, drawn to scale. Inset: Rotationally averaged reconstruction of electron micrographs of purified hook-basal bodies. Compare Table A.3. The signaling molecule CheY-P, which binds FliM, is shown at the lower left. FlgM (lower right) blocks the activity of a sigma-factor that activates late genes. FlgM is pumped out of the cell via the transport apparatus once the basal part of the motor is complete. (Image reconstruction courtesy of David DeRosier, Brandeis University.)

E. Coli in Motion, Howard C. Berg 2004

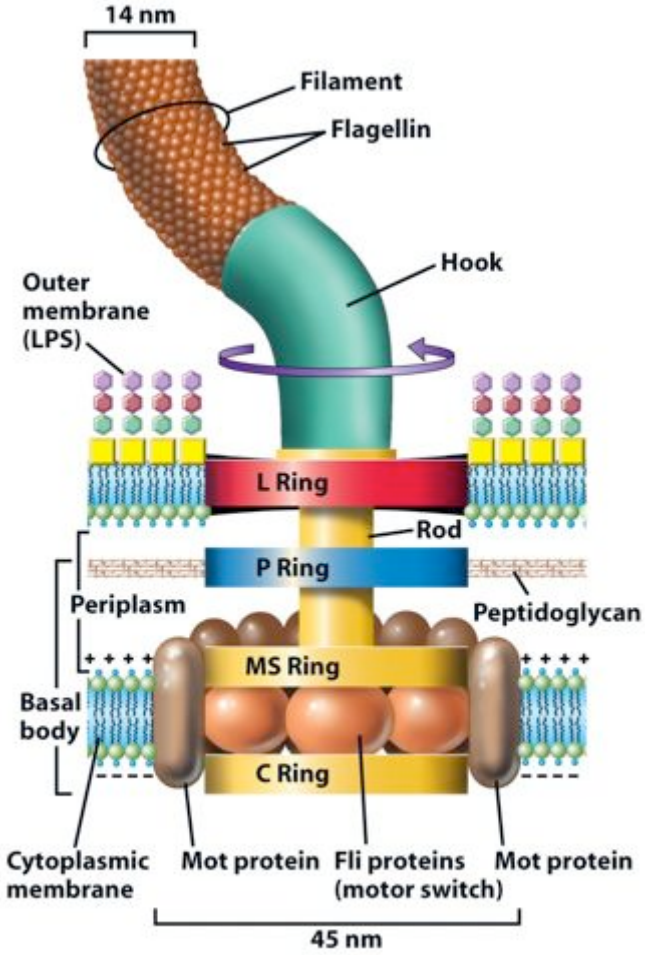

Figure 4-56a Brock Biology of Microorganisms 11/e
© 2006 Pearson Prentice Hall, Inc.

Motor:
proton-driven or
sodium-driven

Propulsion by cilia

• Cilia have many functions: **locomotion**, excretion, circulation, feeding, irritability, contractility, reproduction

• Structure: same as the eukaryotic flagellum (9+2)

• Basic idea: a “Stokesian parachute”

• Metachronal waves

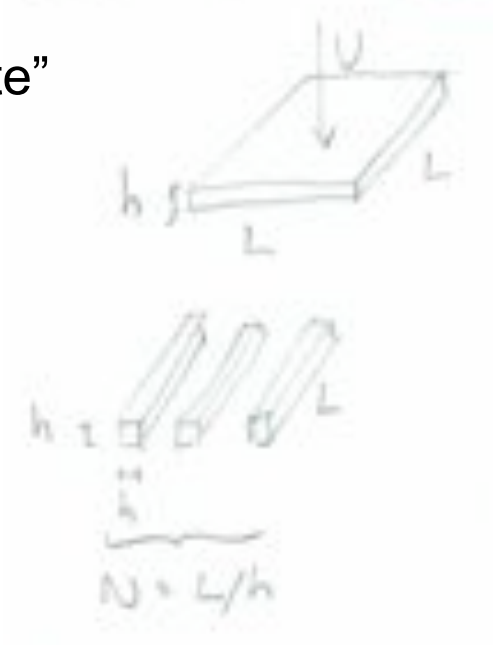

Propulsion by cilia

Paramecium

Figure 2-23c Brock Biology of Microorganisms 11/e

Propulsion by cilia

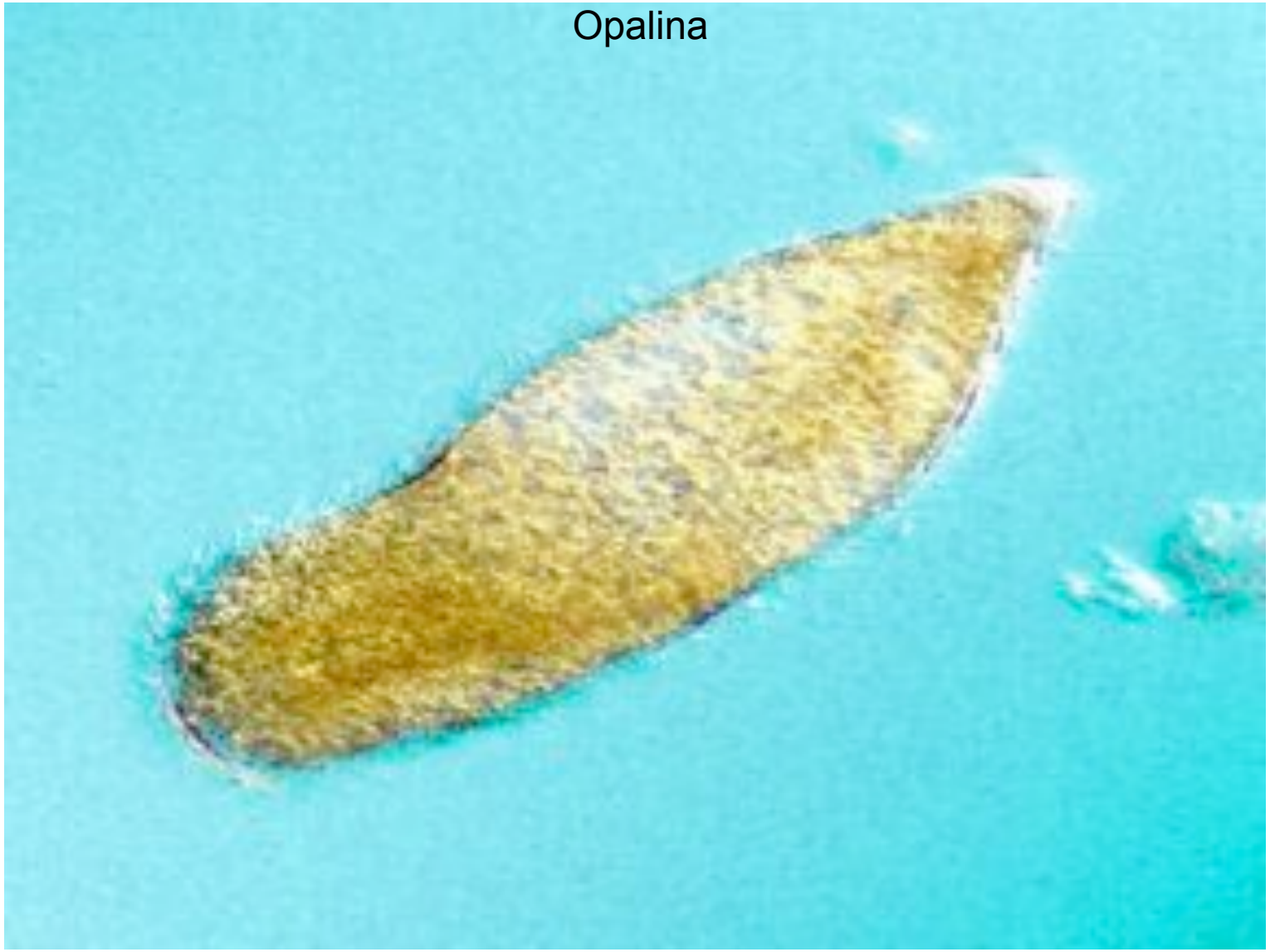

Cilia : metachronal waves

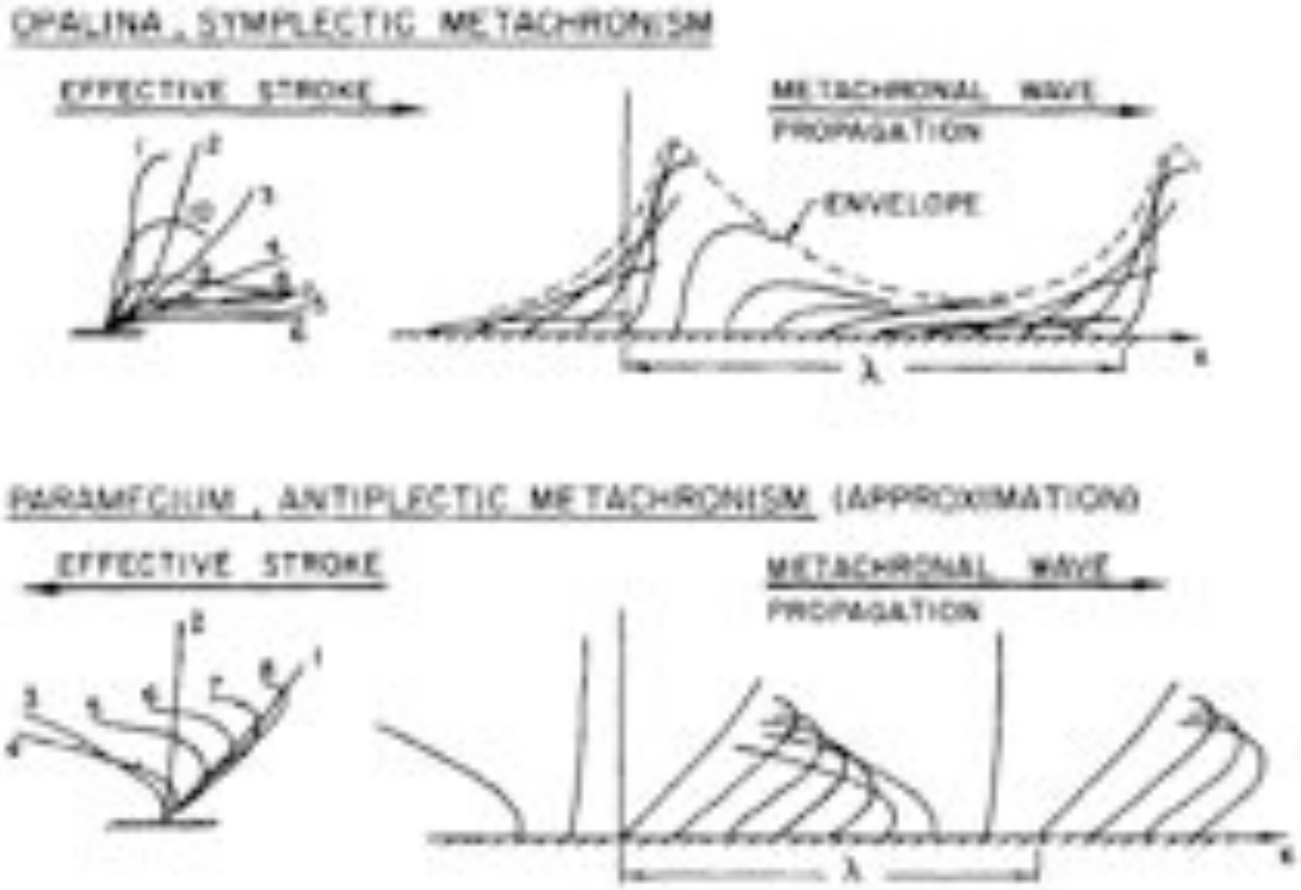

Figure 16 Approximate beat patterns for *Opalina* and *Paramecium* with the positions of an individual cilium at equal intervals in time on the left and the positions of an array of cilia at a given time on the right, showing the symplectic metachronism of *Opalina* and an antiplectic approximation to the metachronism of *Paramecium*.

Brennen&Winet, Ann. Rev. Fluid Mech. 1977

Metachronal waves

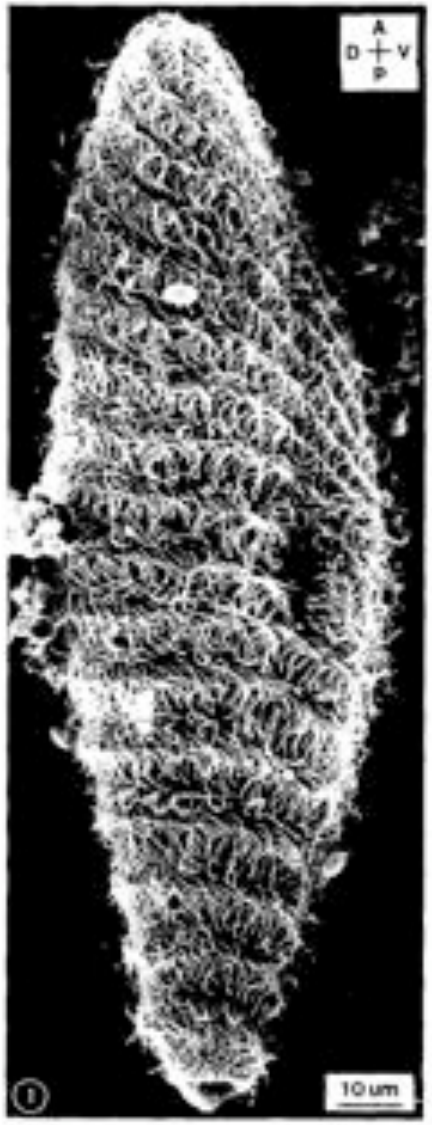

Figure 15 A scanning electron micrograph following rapid fixation of the ciliated protozoan *Paramecium* (from Tamm 1972). The metachrony of this specimen is dexioplectic and/or antiplectic. A-P, anterior-posterior axis; D-V, dorsal-ventral sides. (We are indebted to Dr. S. L. Tamm for this photograph.)

Brennen&Winet, Ann. Rev. Fluid Mech. 1977

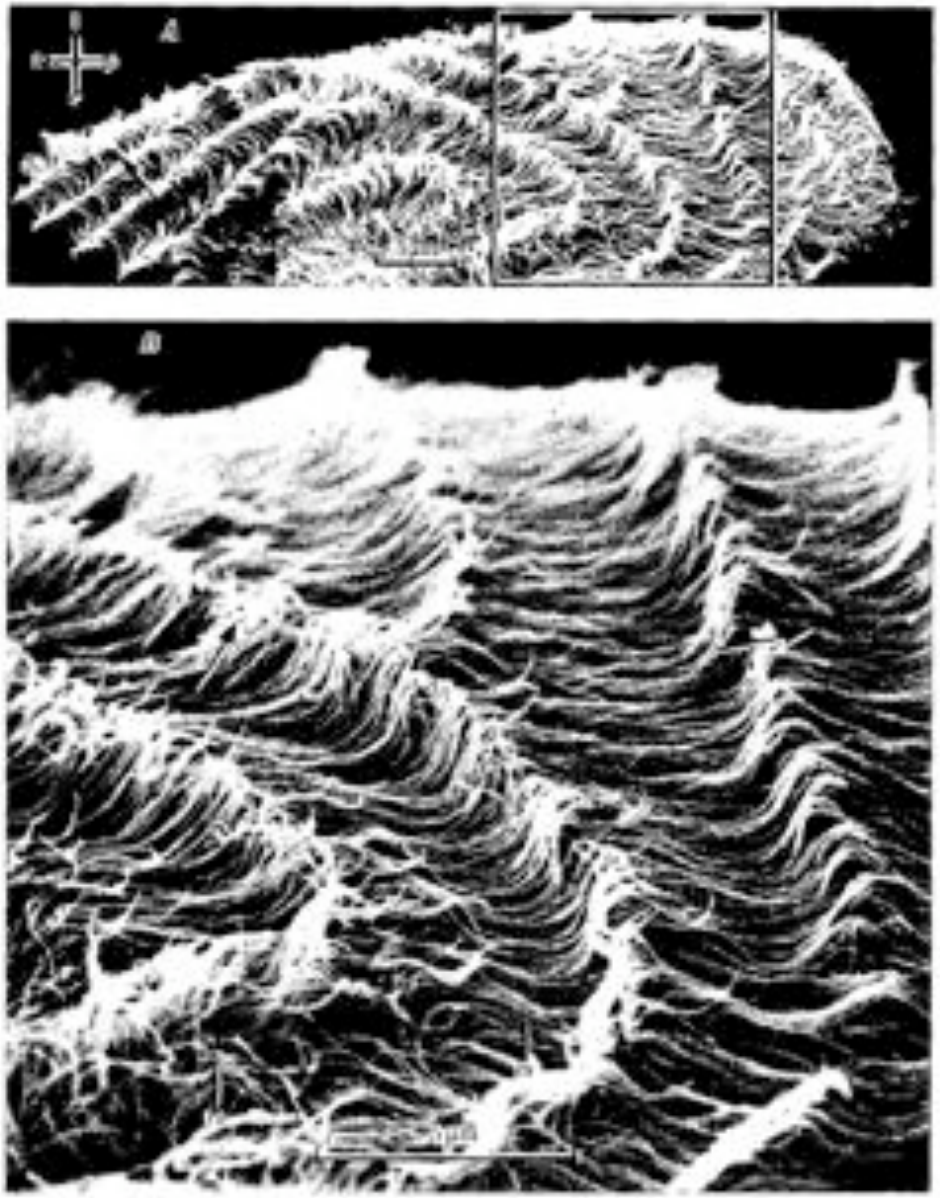

Figure 14 A scanning electron micrograph following rapid fixation of the ciliated protozoan *Opalina* (from Tamm & Horridge 1970). As in the preceding figure, the in vivo metachronal wave orientation is reflected in the pattern over the fixed specimen. Arrows indicate the directions of the metachronal wave. The key difference between the two specimens is that this figure is limited to all or part of a single cell. (We are indebted to Dr. S. L. Tamm for this photograph.)

Brennen&Winet, Ann. Rev. Fluid Mech. 1977

Energetic cost of swimming

- Power required for swimming ~ square of swimming speed
  (huge cost increase for fast swimmers, e.g. Mitchell)

- Efficiency: only ~1% !!

- Conversion:
  1 Joule ~ 5×10^7 glucose molecules

- A Datsun in Saudi Arabia??
  (Purcell 1977)

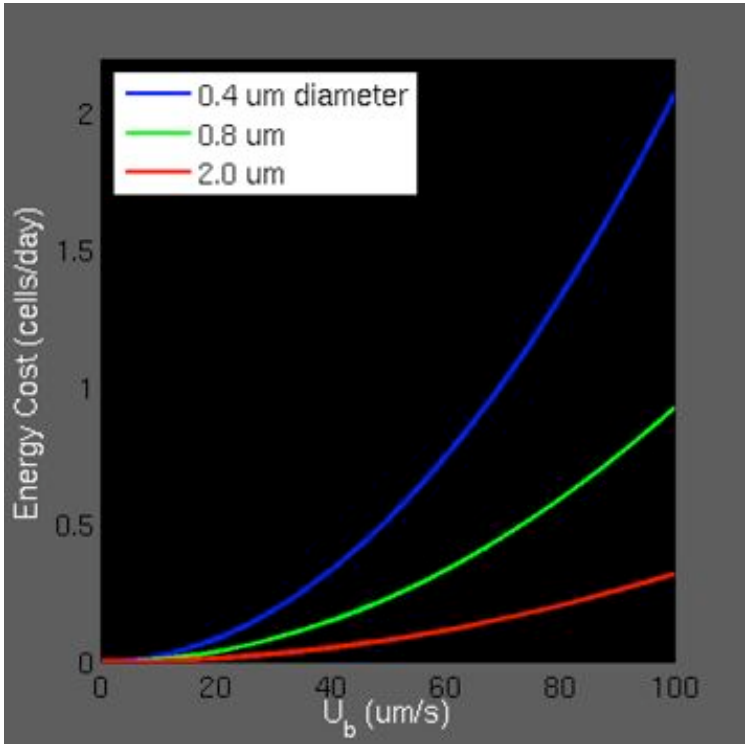

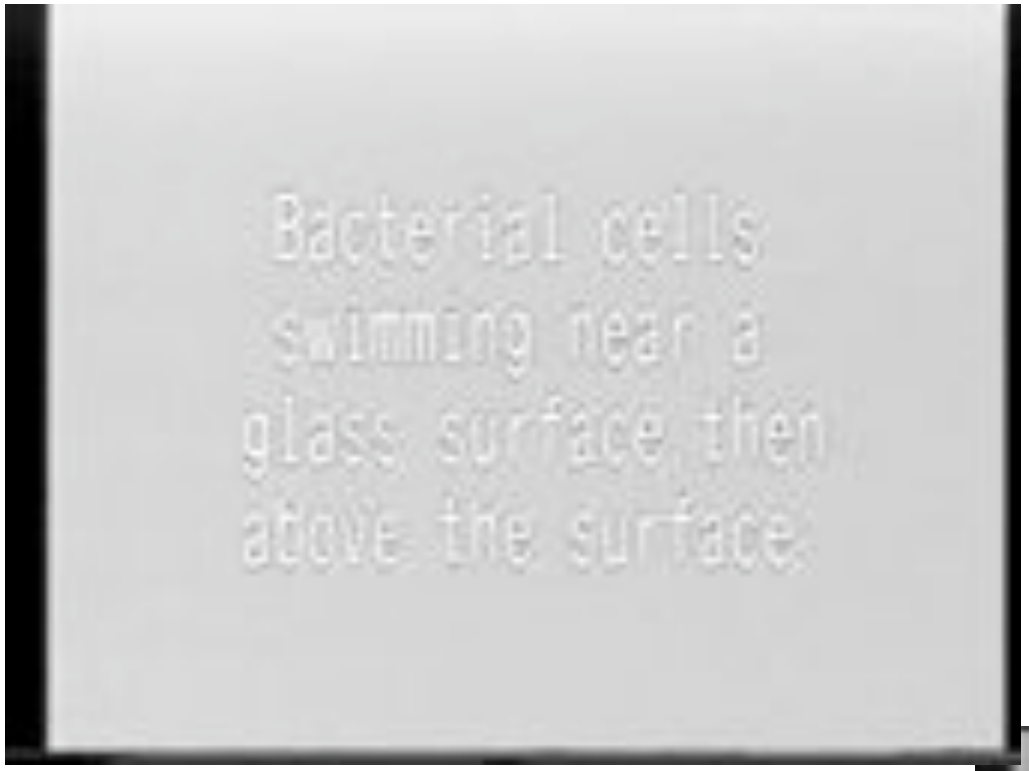

Escherichia coli swimming

(H. Berg)

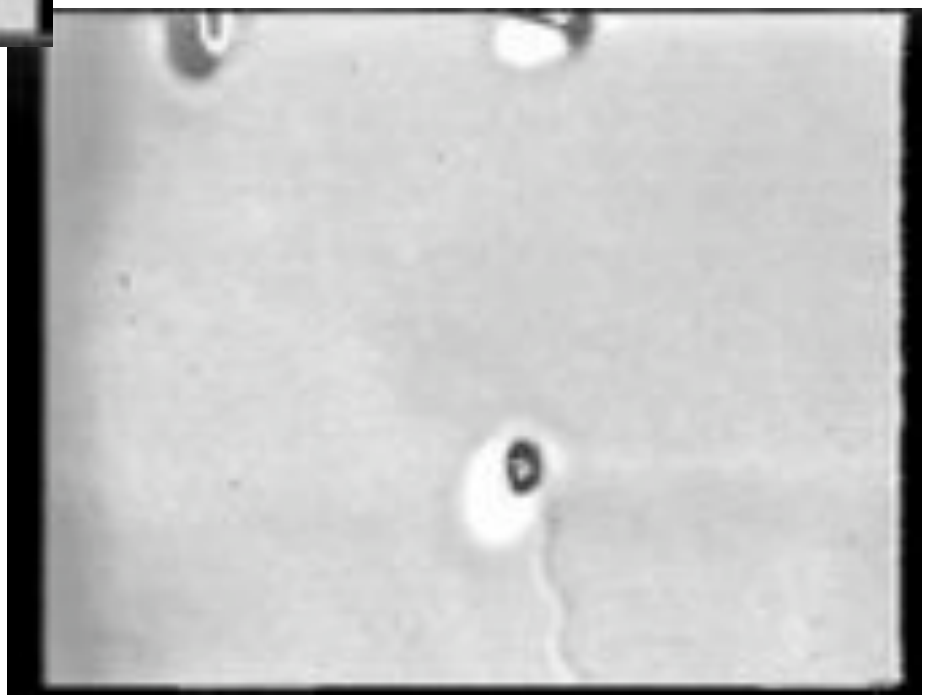

Bacteria

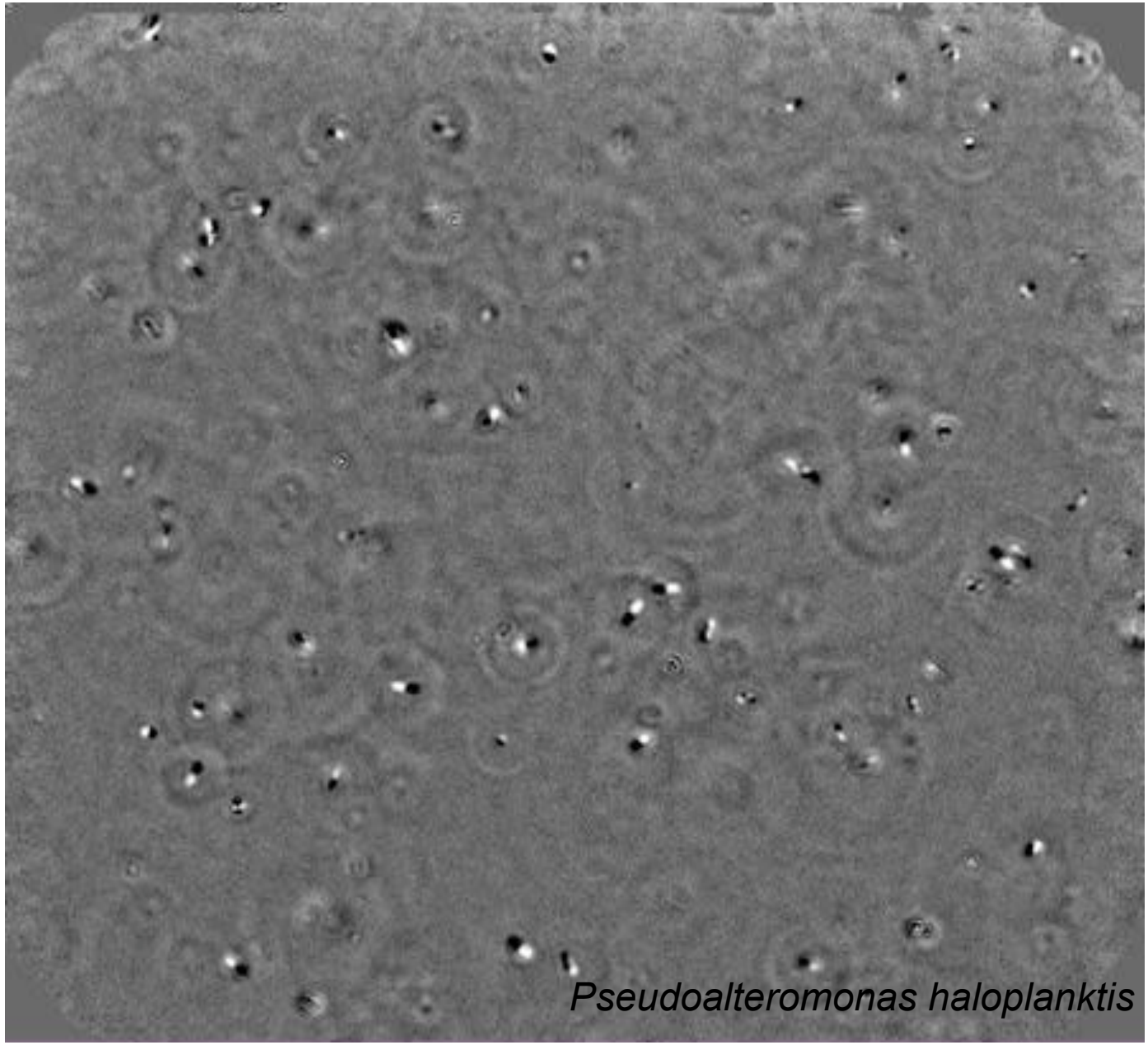

Berg's 3D tracking microscope

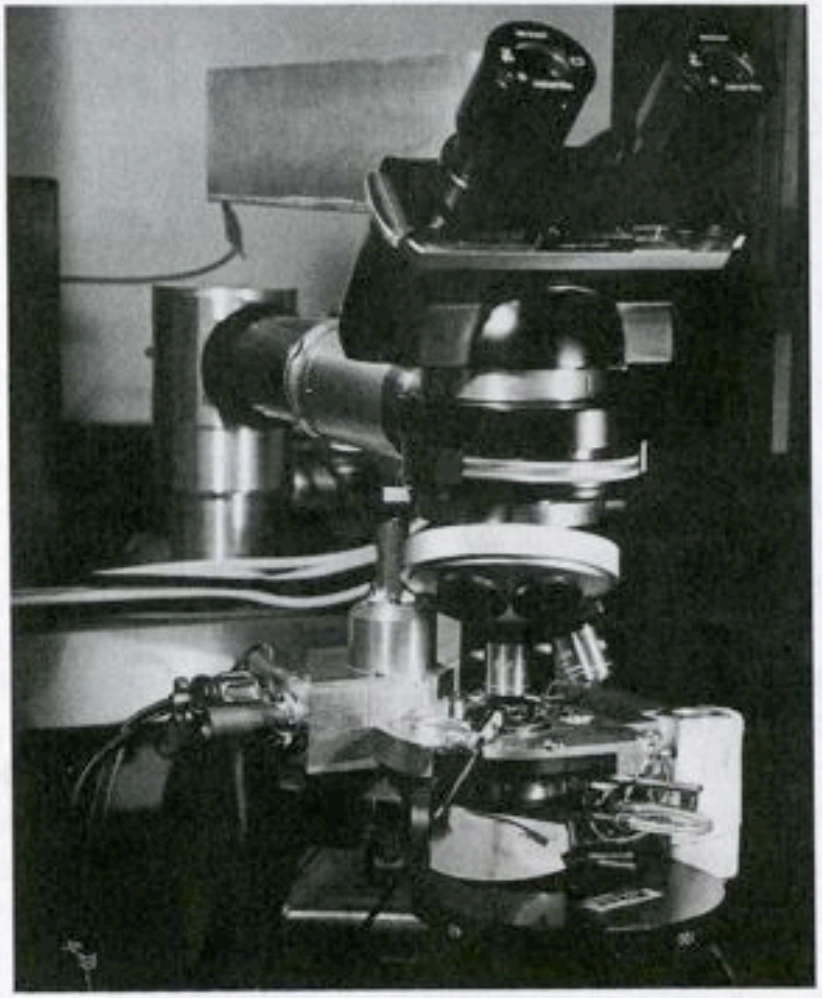

FIGURE 4.1. The tracking microscope, circa 1974. The lenses, mirrors, and fiber-optic assembly used to dissect the image of a cell was built into the rectangular box extending back from the top of the binocular. Just below the objective is a thermostatted enclosure containing a small chamber in which the bacteria were suspended, mounted on a platform driven by three sets of electromagnetic coils (similar to loudspeaker coils) built into the assembly at the left. (From Berg, 1978, Fig. 2).

The flagellar bundle → a ‘run’

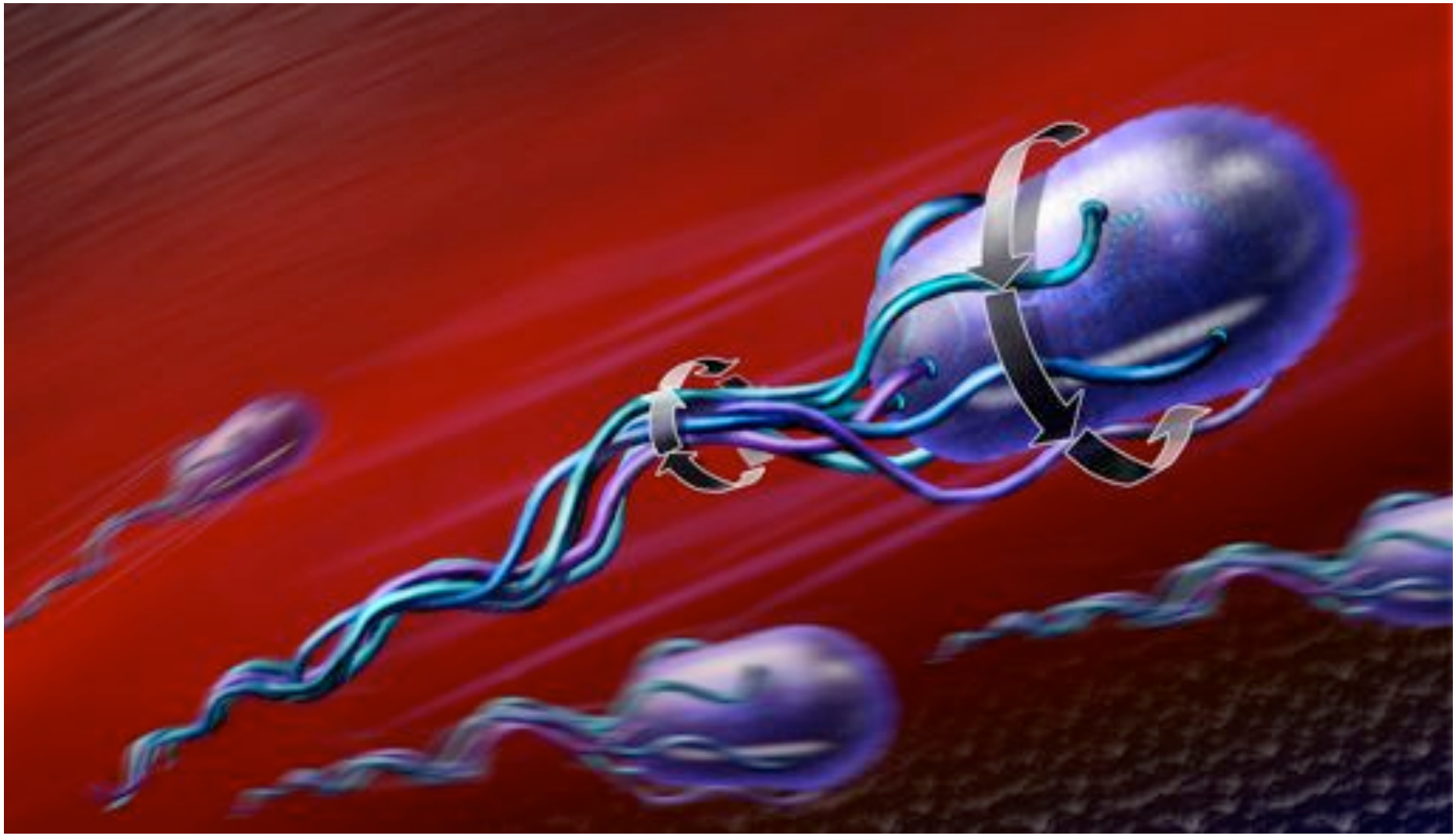

http://en.wikipedia.org/wiki/Flagella

E. coli's 'run and tumble' swimming

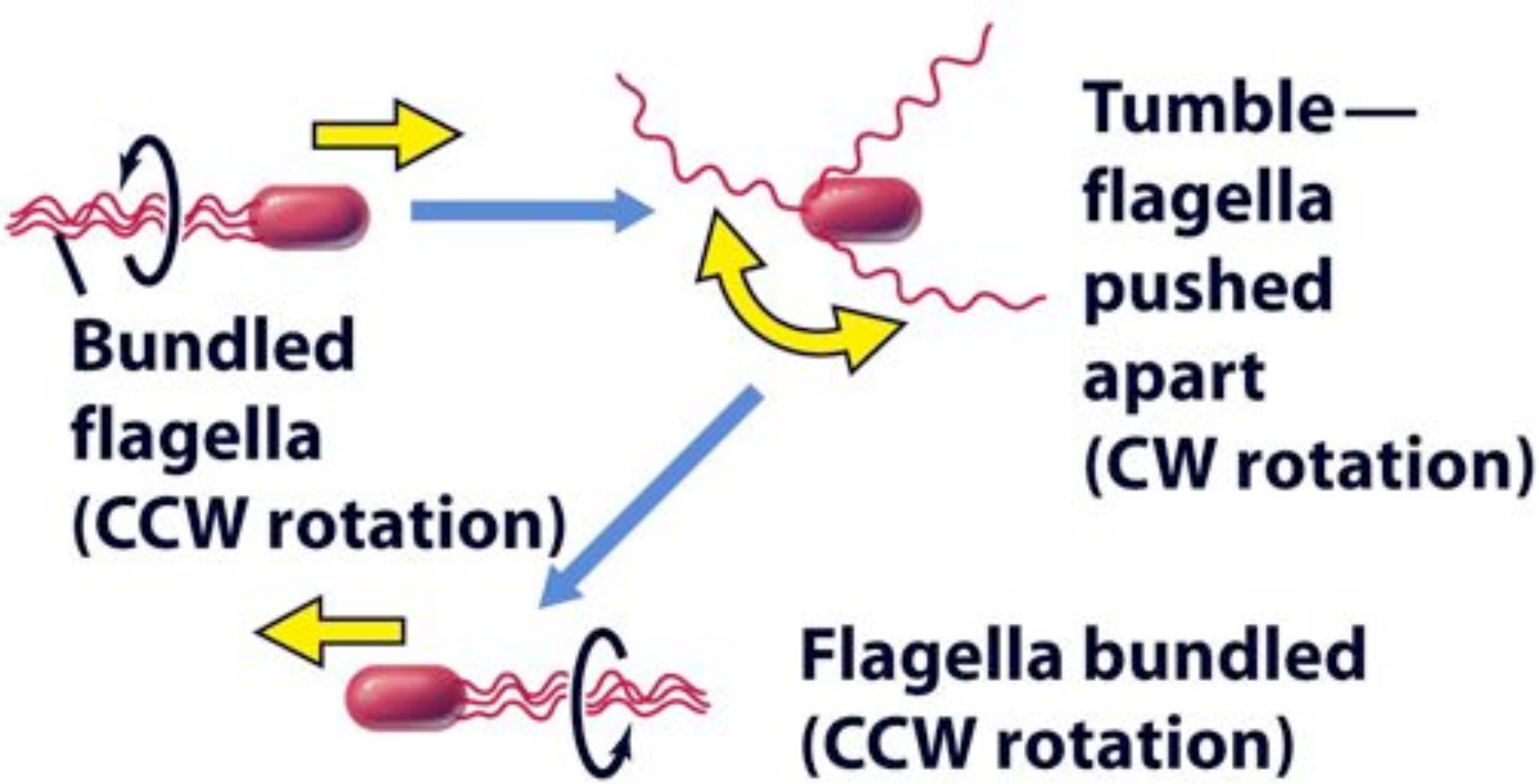

Peritrichous

Figure 4-58a Brock Biology of Microorganisms 11/e

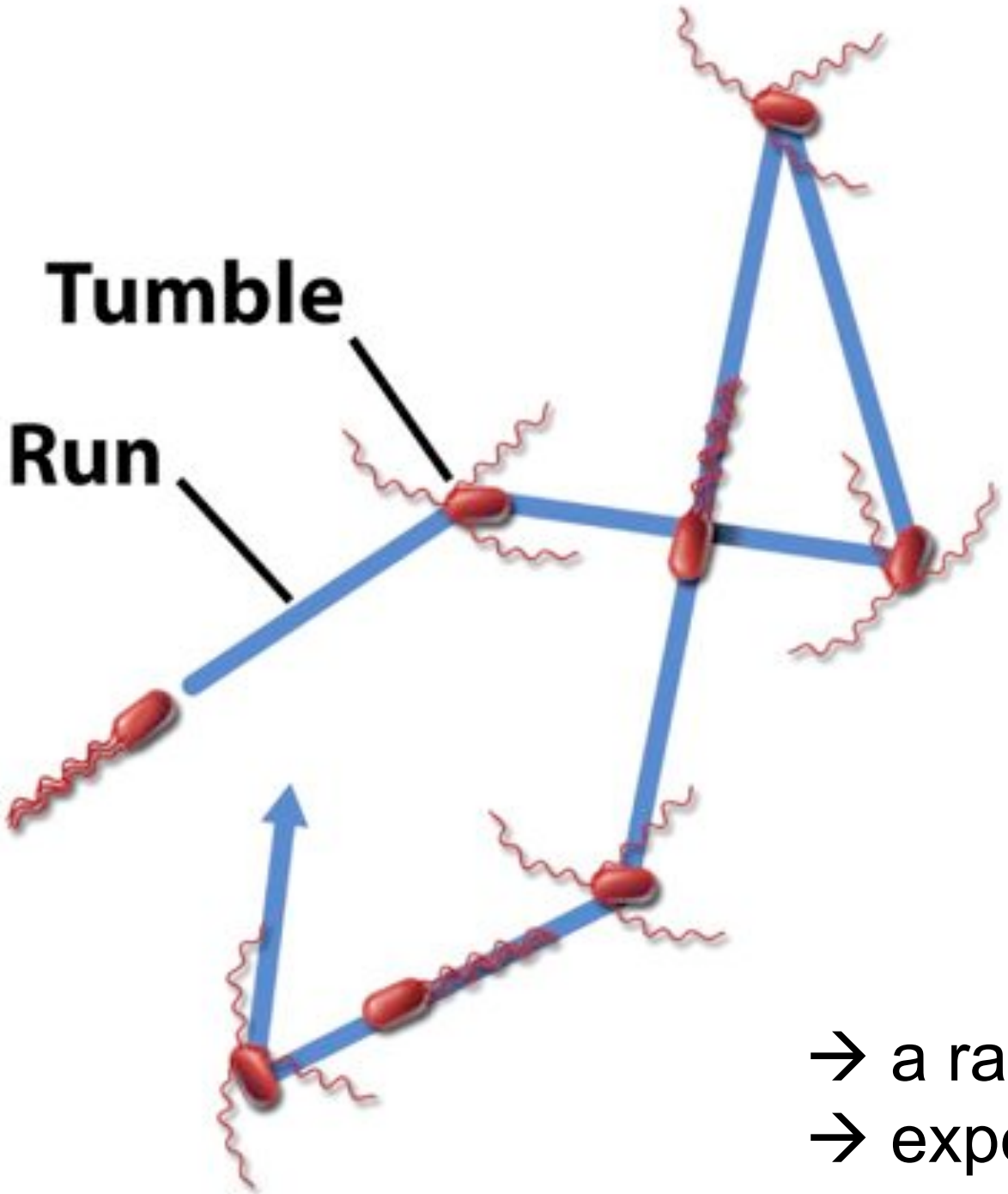

→ a random walk!
→ expect diffusion

A population of bacteria “diffuses”

(time scale 15 min; length scale 1 mm)

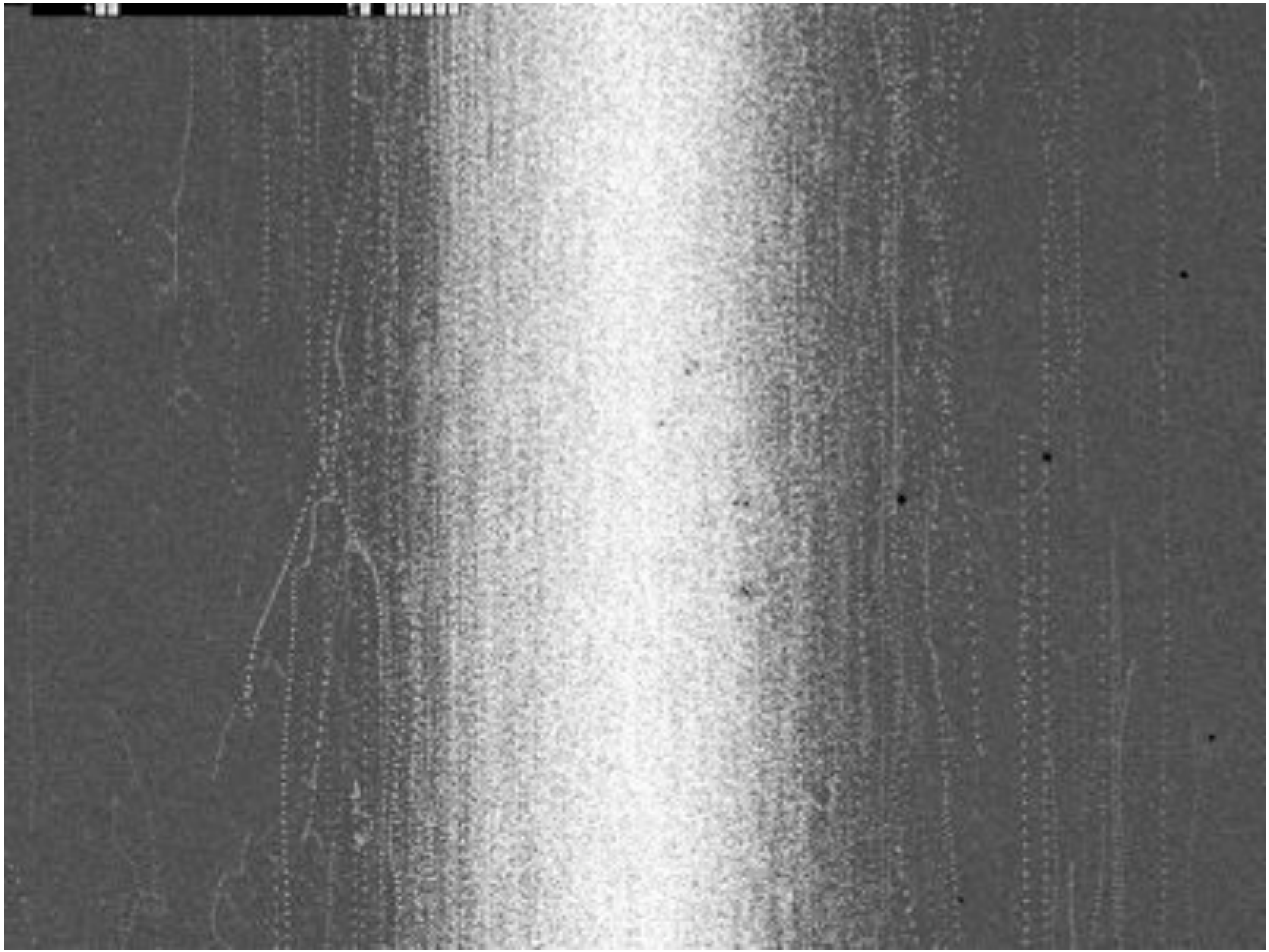

A population of bacteria “diffuses”

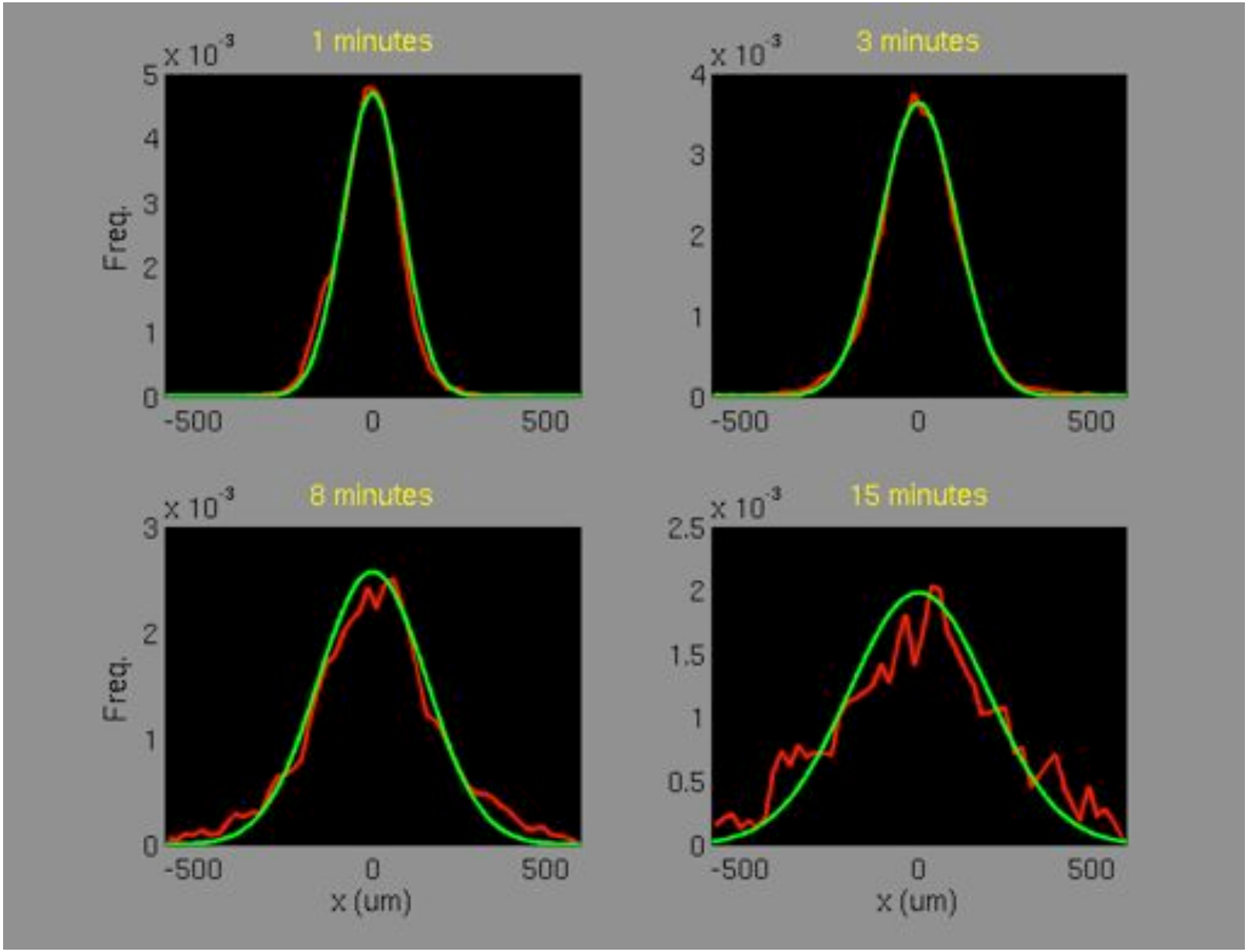

Diffusion coefficient D = 0.5 x 10^{-10} m^2/s

Run-and-tumble

E. coli's flagella are in fact polymorphic

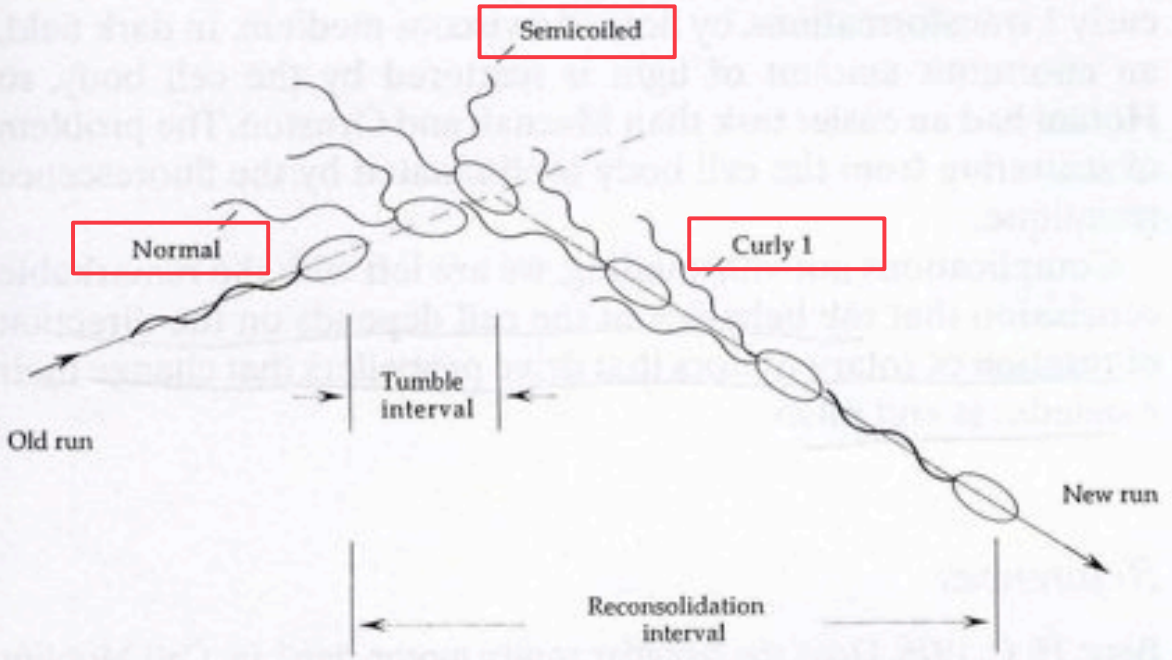

FIGURE 5.6. A schematic drawing of the events that usually occur during a tumble. A cell with a bundle of two flagellar filaments is shown swimming from left to right. The cell alters course as the motor driving one filament changes its direction of rotation and the filament undergoes a normal to semicoiled transformation. This change in course defines the tumble interval, which, according to both the tracking and video data, takes 0.14 second, on average. As the cell begins to move along its new track, the filament undergoes a semicoiled to curly 1 transformation. Both the normal and curly 1 filaments generate forward thrust, but the curly one at a smaller magnitude. Finally, after the direction of flagellar rotation changes again, the filament reverts to normal. As it does so, it rejoins the bundle, and the cell resumes its initial speed. The time from the initial disruption of the bundle to its reconsolidation is defined as the reconsolidation interval. According to the video data, this takes 0.43 second, on average.

E. Coli in Motion. Howard C. Berg 2004

Other strategies

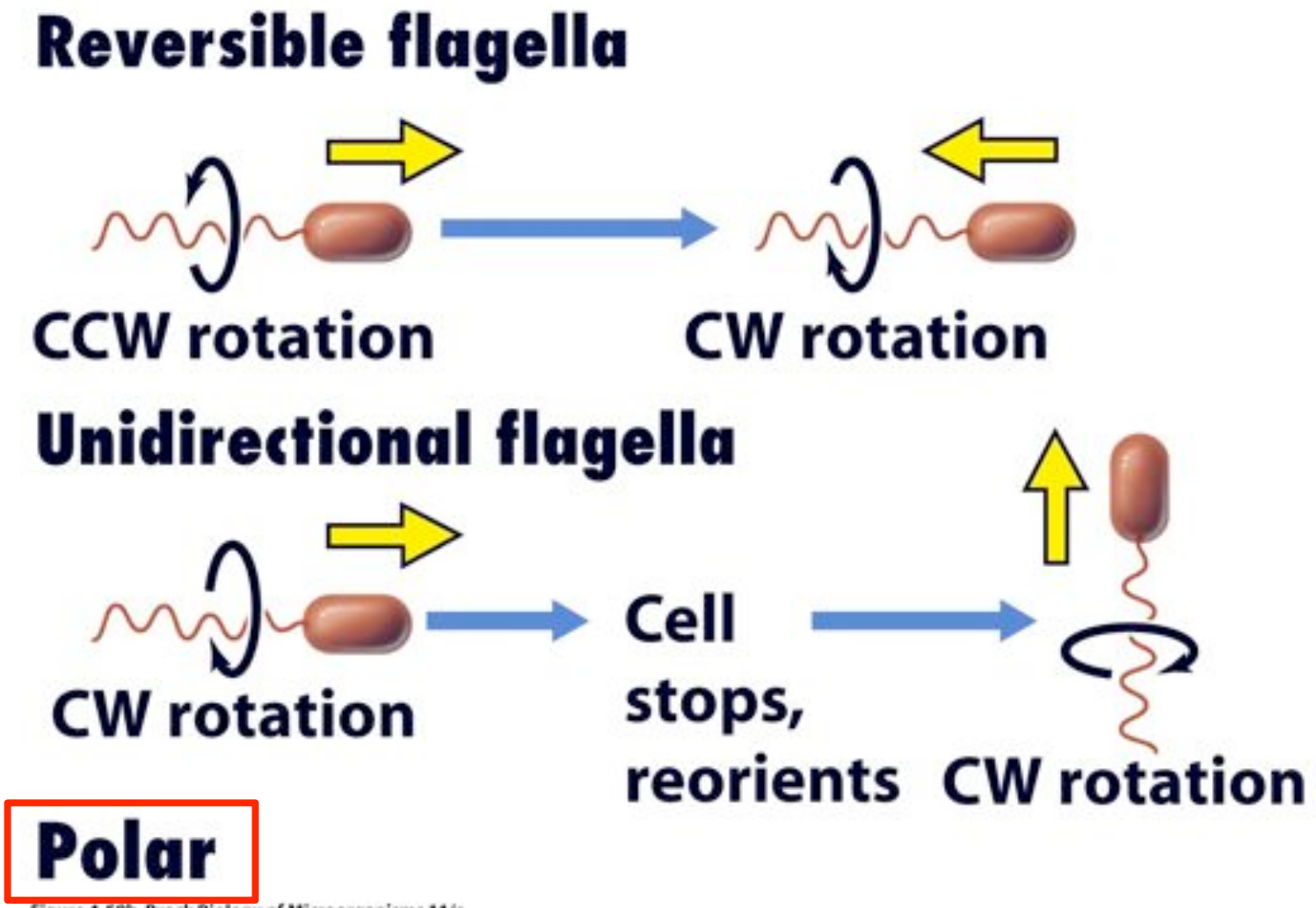

Figure 4-58b Brock Biology of Microorganisms 11/e

Different swimming behaviors (mutants)

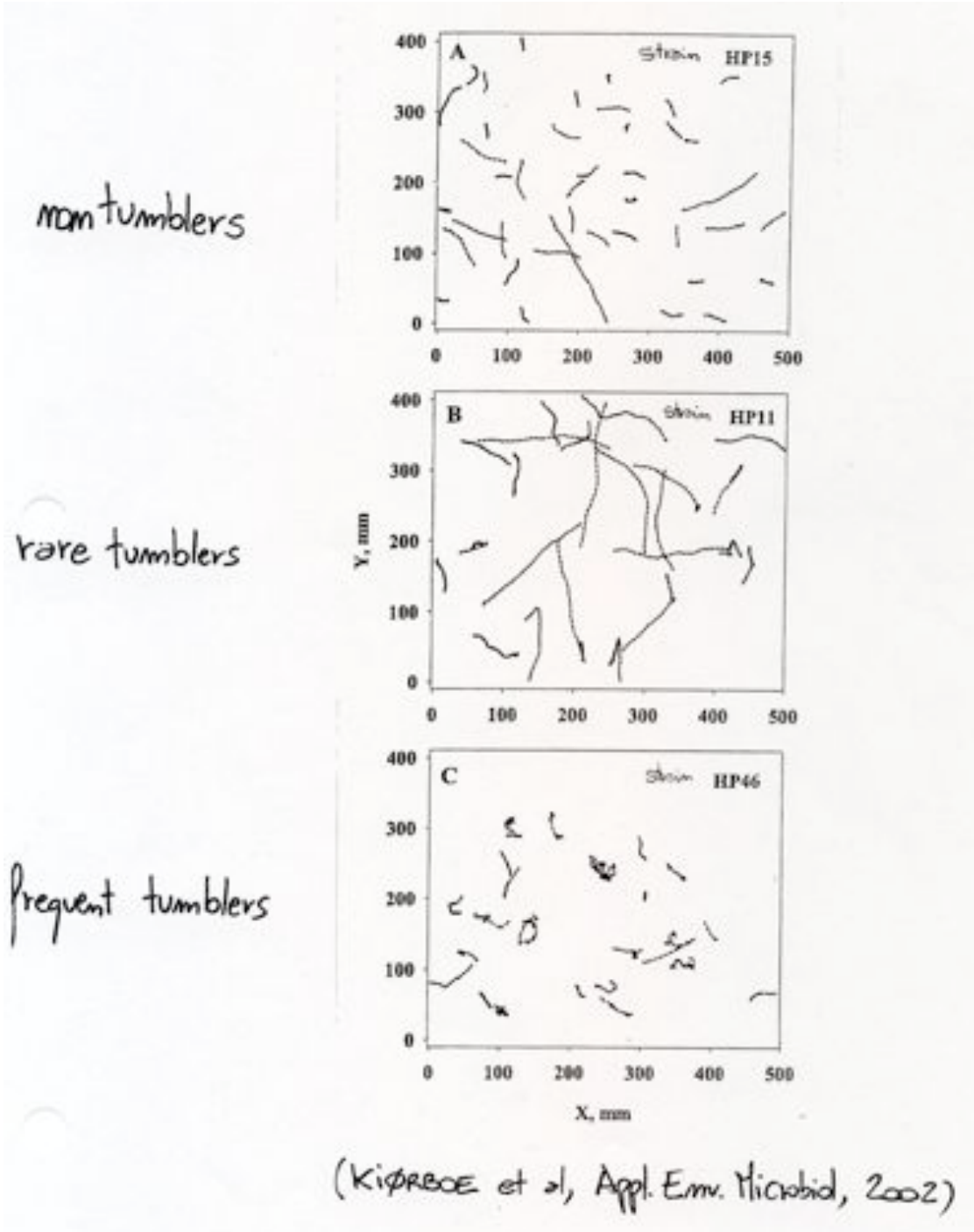

Synechococcus swimming

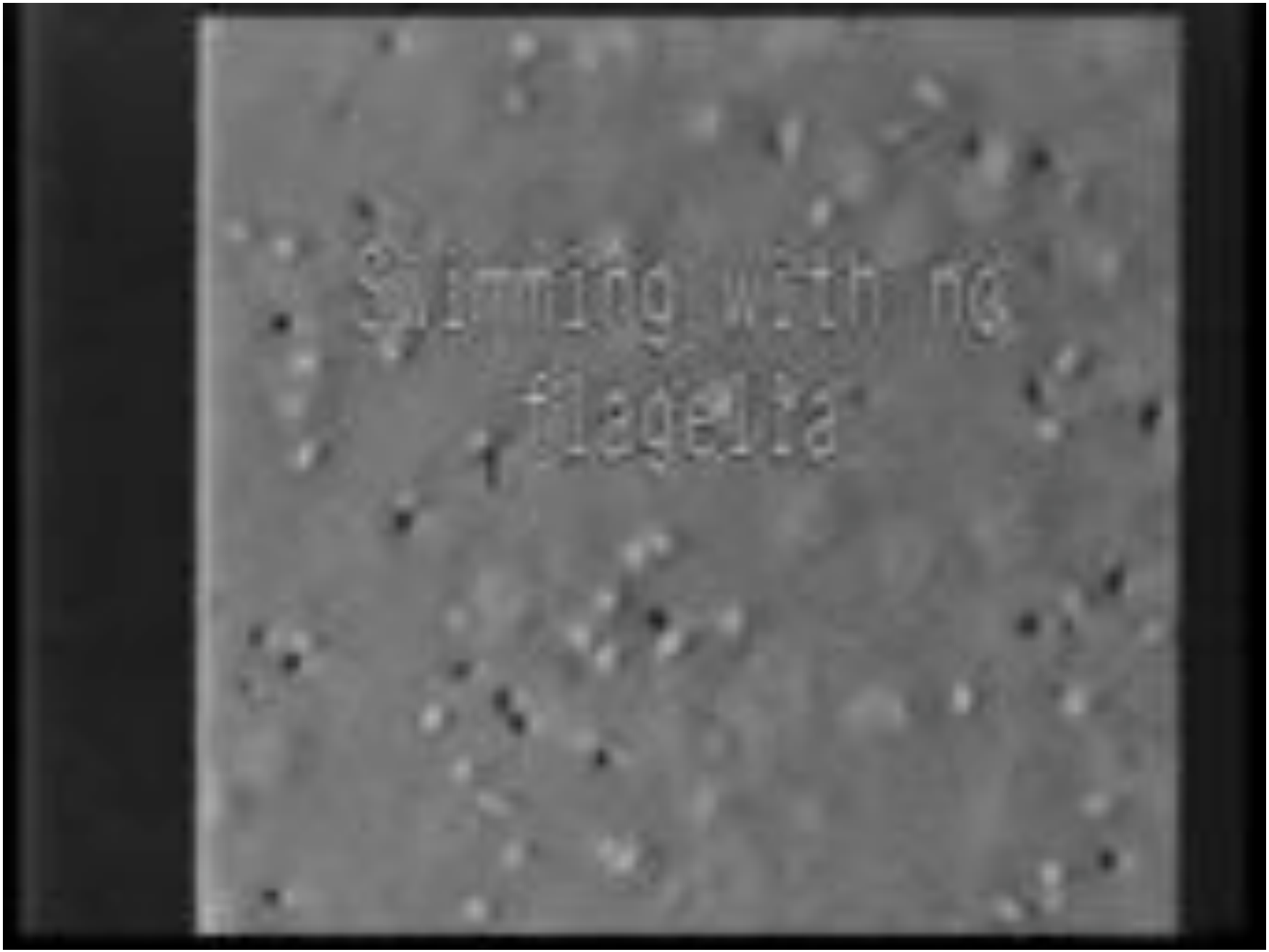

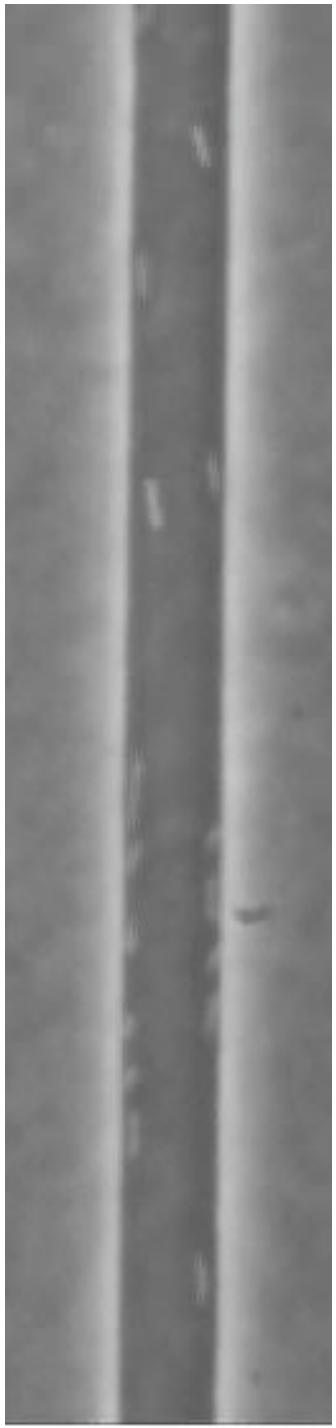

E. Coli swims on the right

(DiLuzio et al, Nature, 2005)

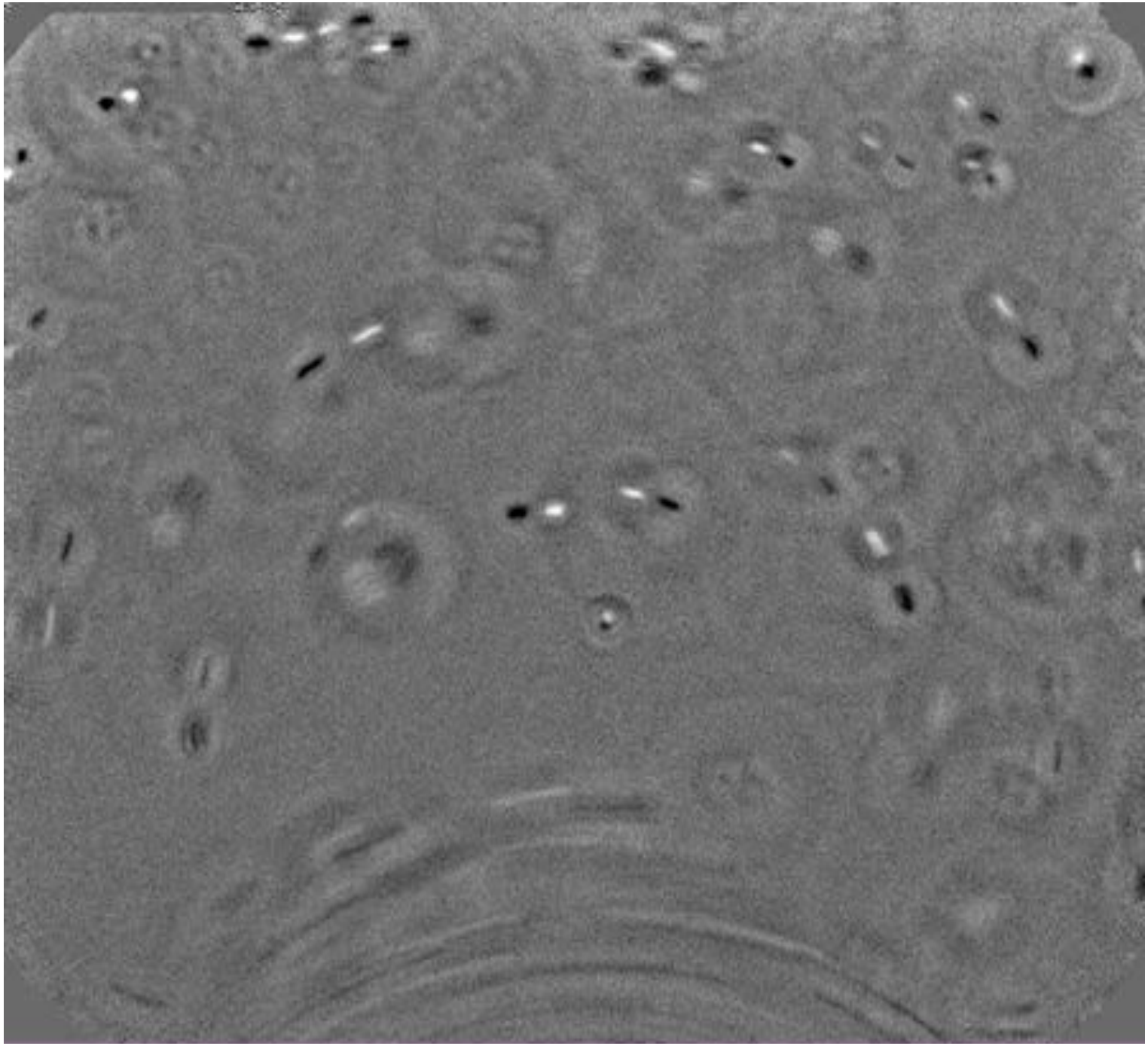

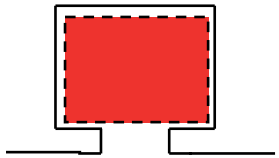

High flow

Marcos & Stocker, 2006

Chemotaxis: introduction

The capillary assay

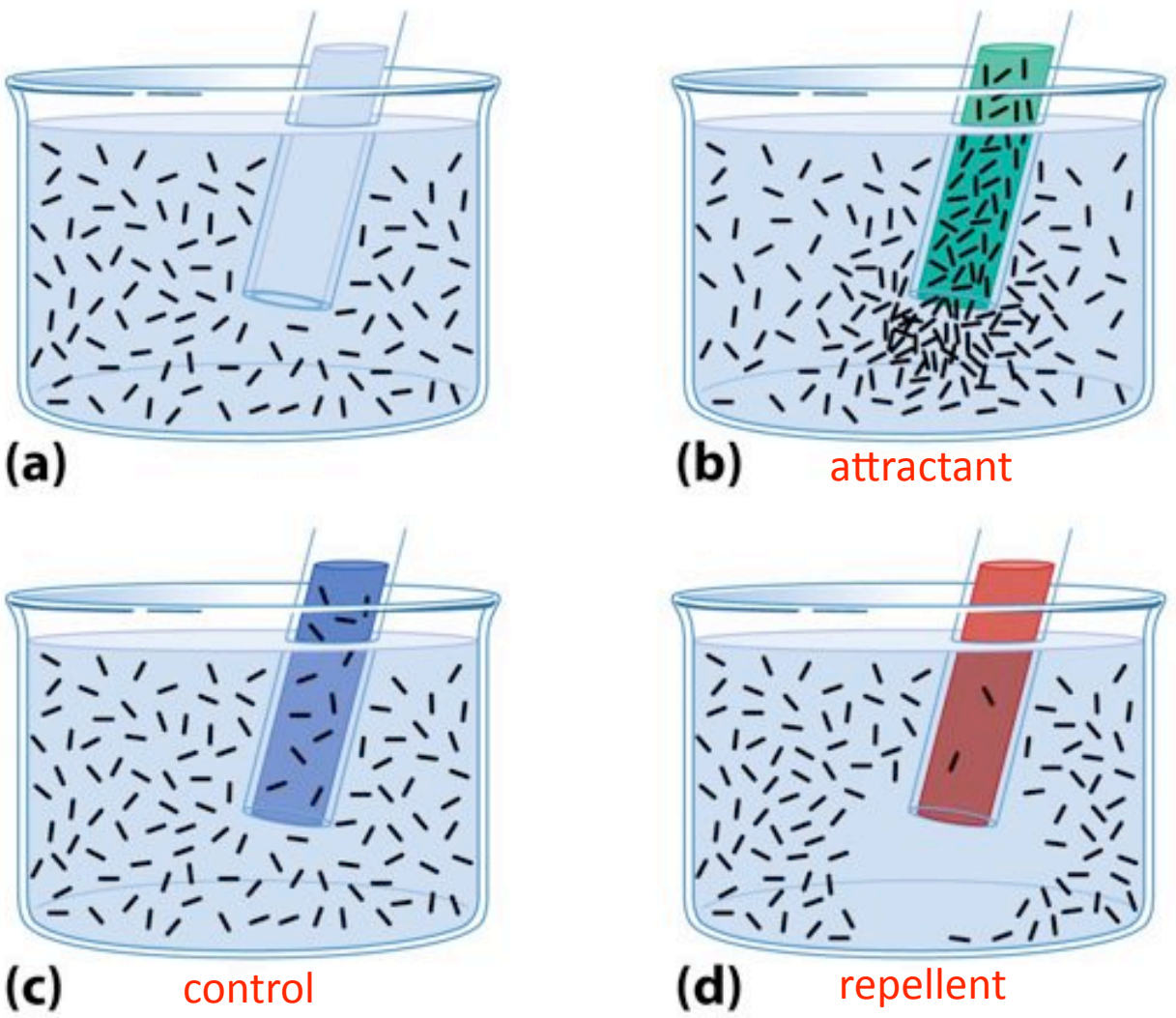

Figure 4-62a-d Brock Biology of Microorganisms 11/e

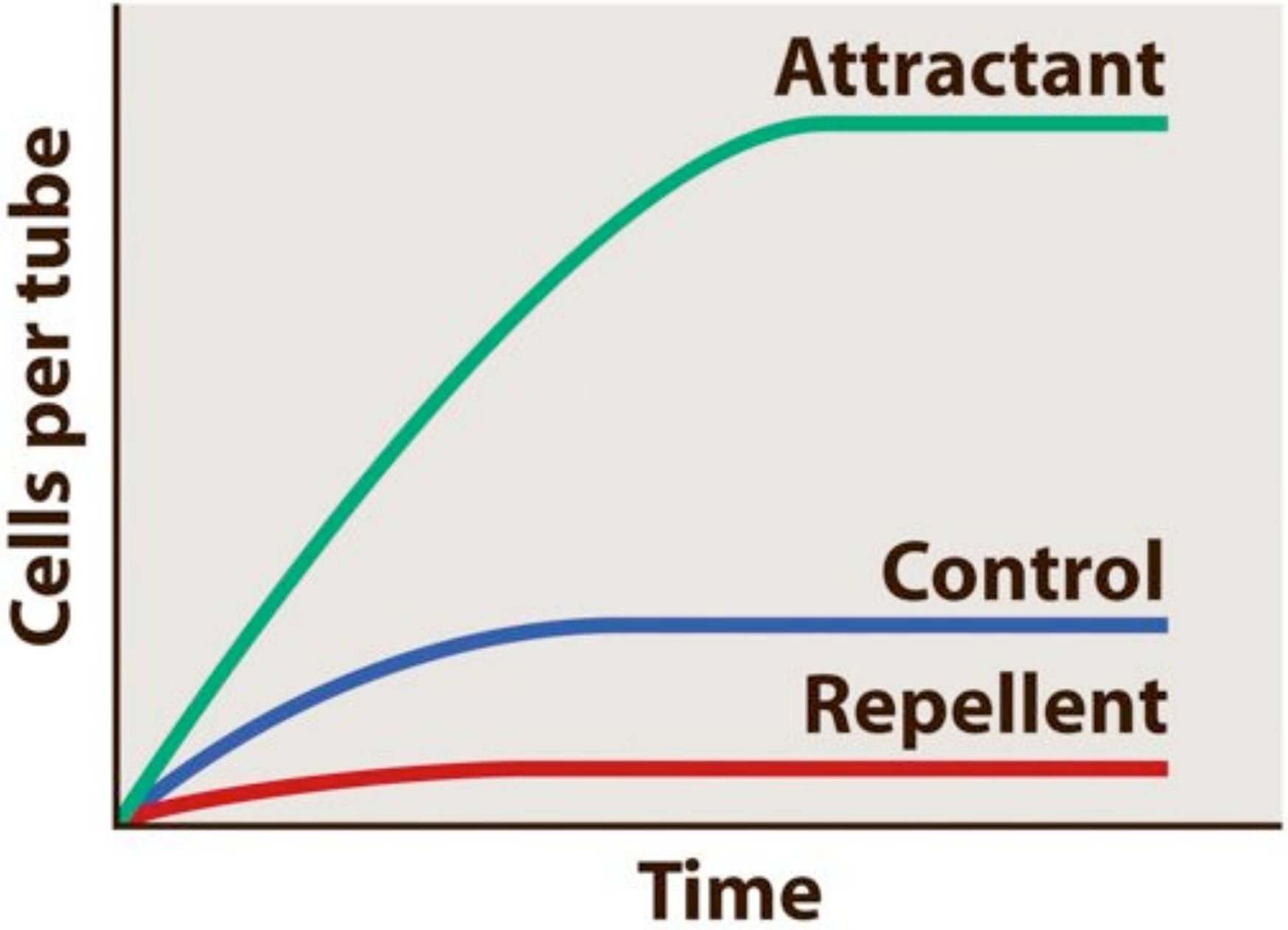

Figure 4-62e Brock Biology of Microorganisms 11/e

Receptors

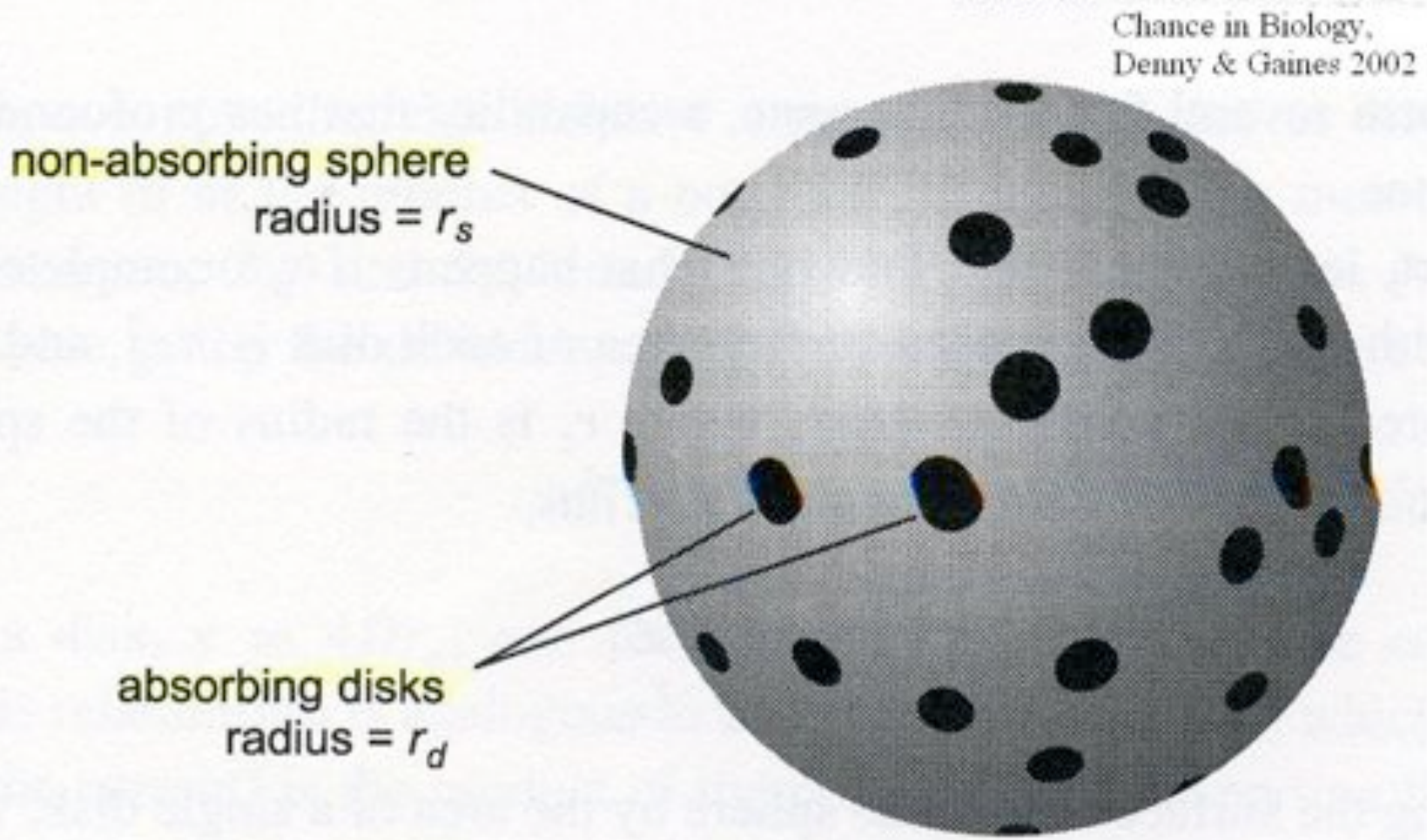

FIG. 5.5 Absorbing disks (a model for receptors or ion channels) scattered on a non-absorbing sphere (a model for a cell).

Chemotaxis in *E. coli:*
delay tumble when conditions are getting better

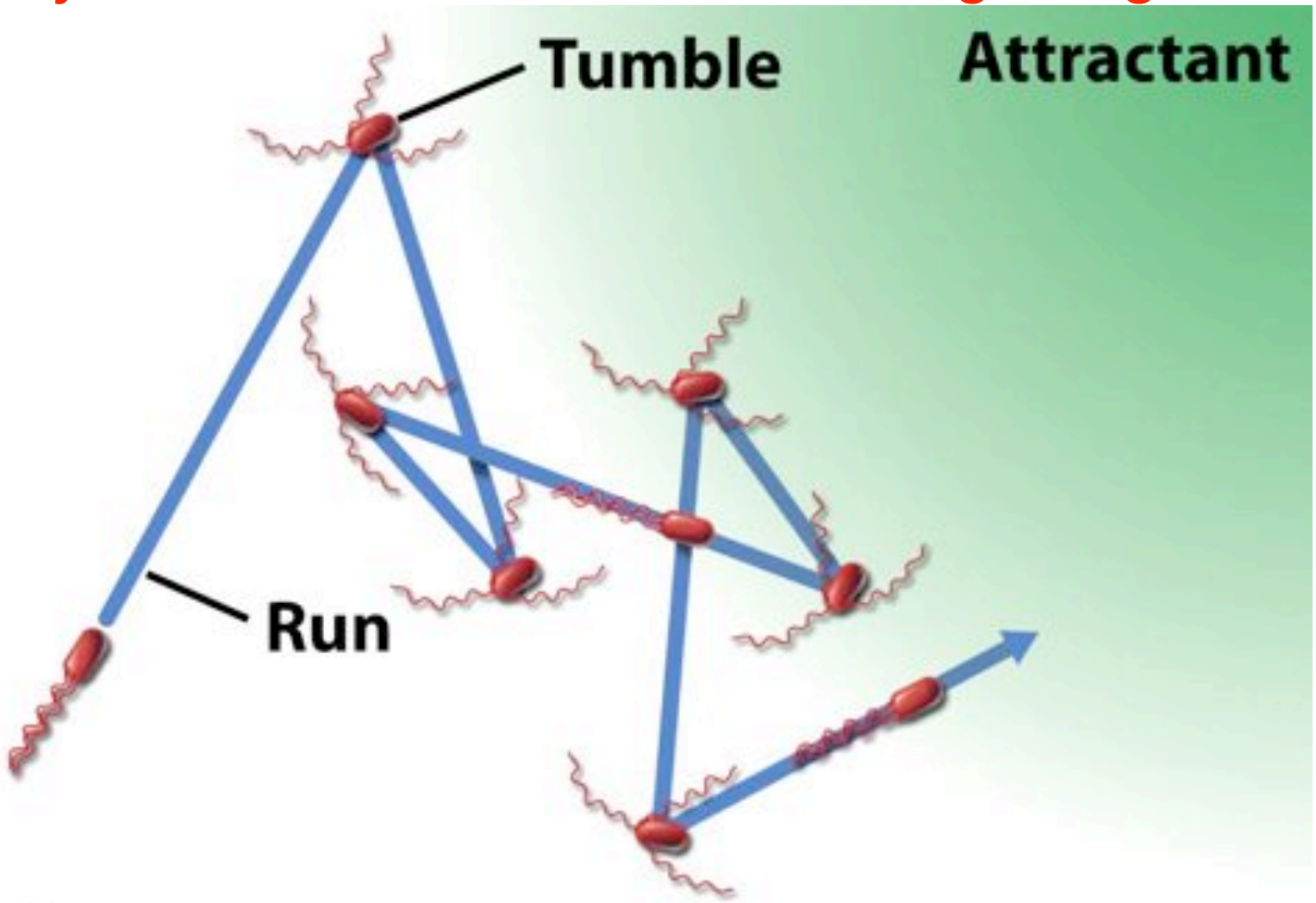

Temporal vs. spatial gradient sensing

Examples of different taxis in bacteria

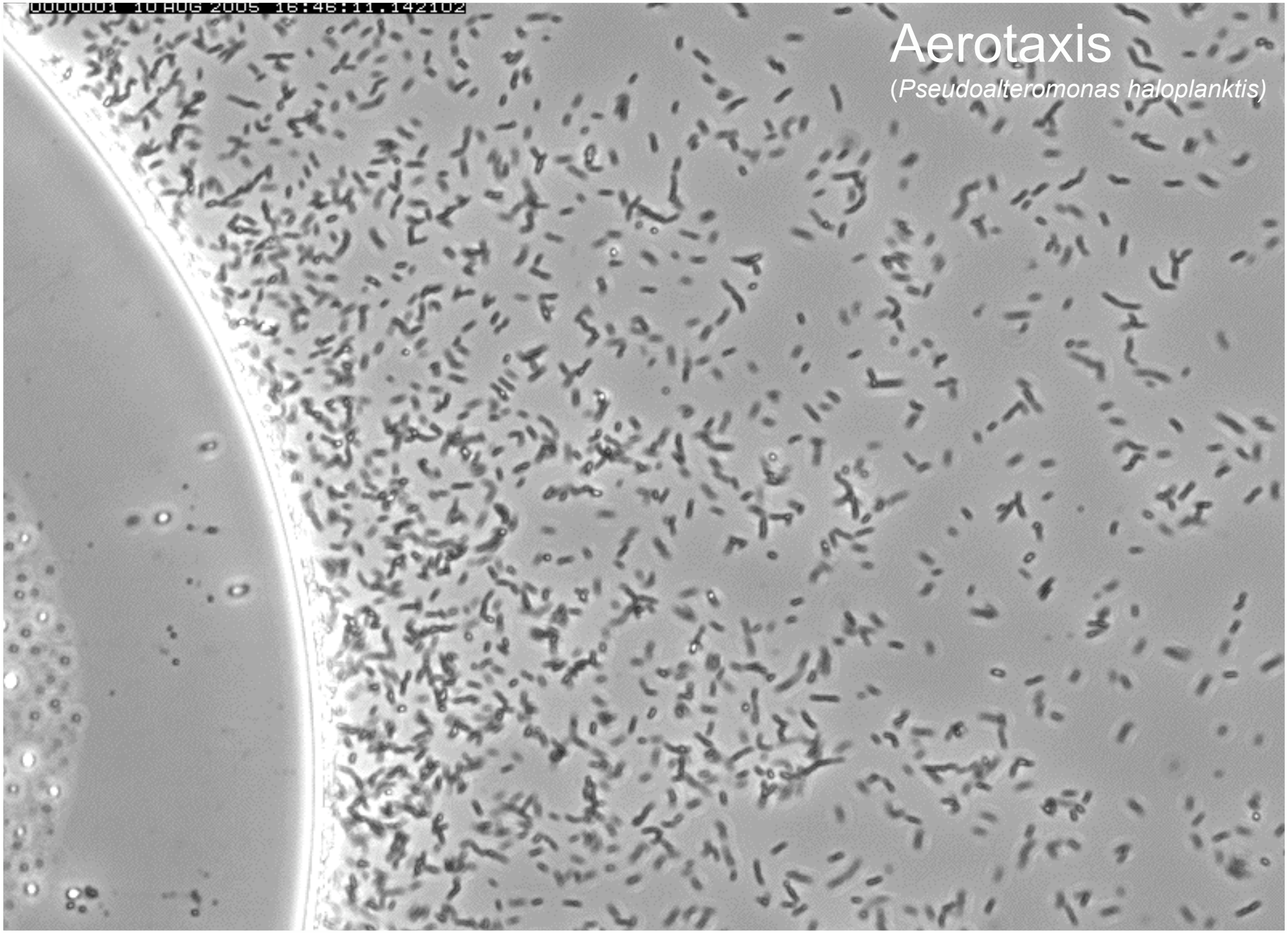

First taxis discovered (Engelmann 1883, while studying photosynthesis)

Aerotaxis

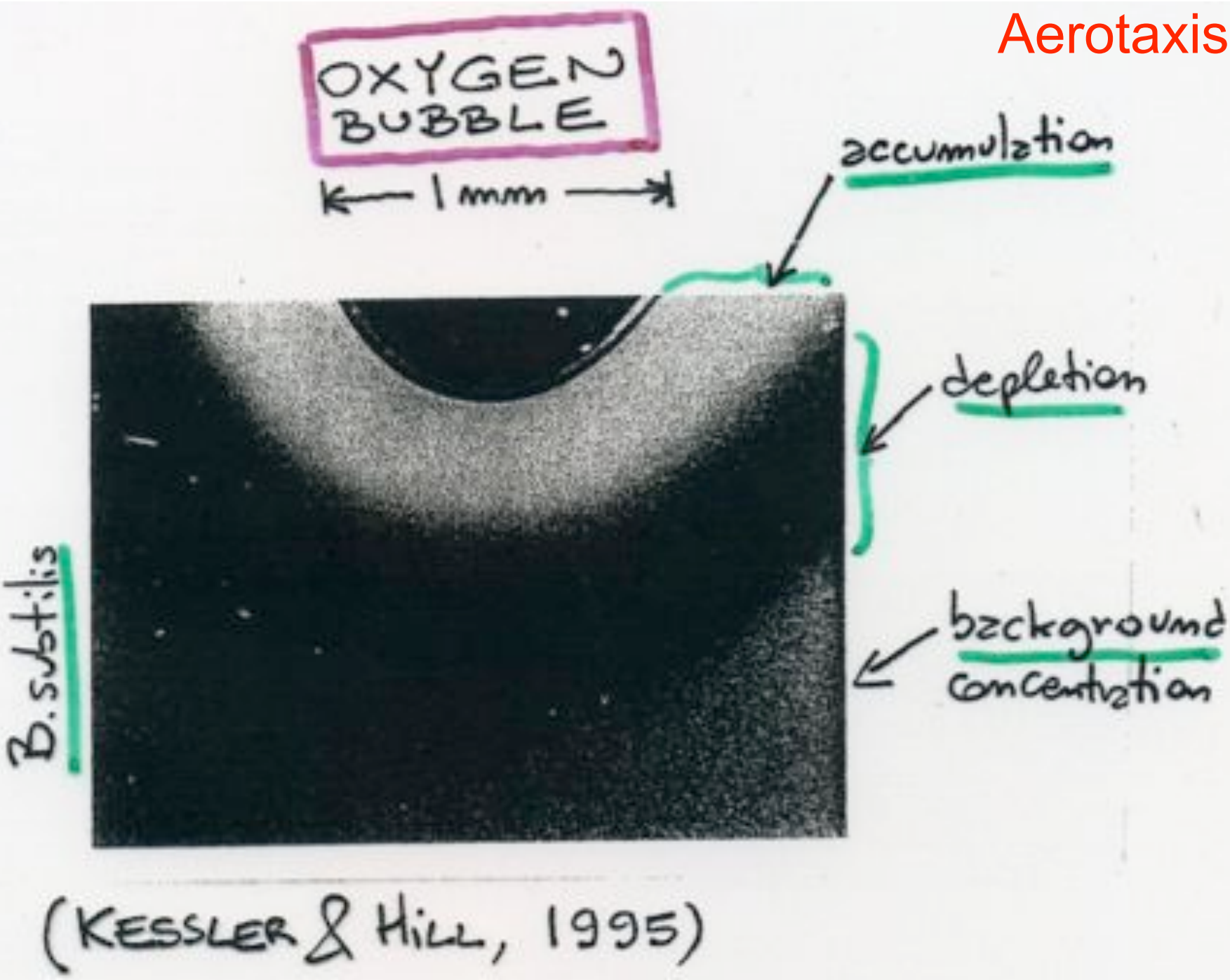
OXYGEN BUBBLE
1 mm
accumulation
depletion
background concentration
B. subtilis
(KESSLER & HILL, 1995)

Phototaxis

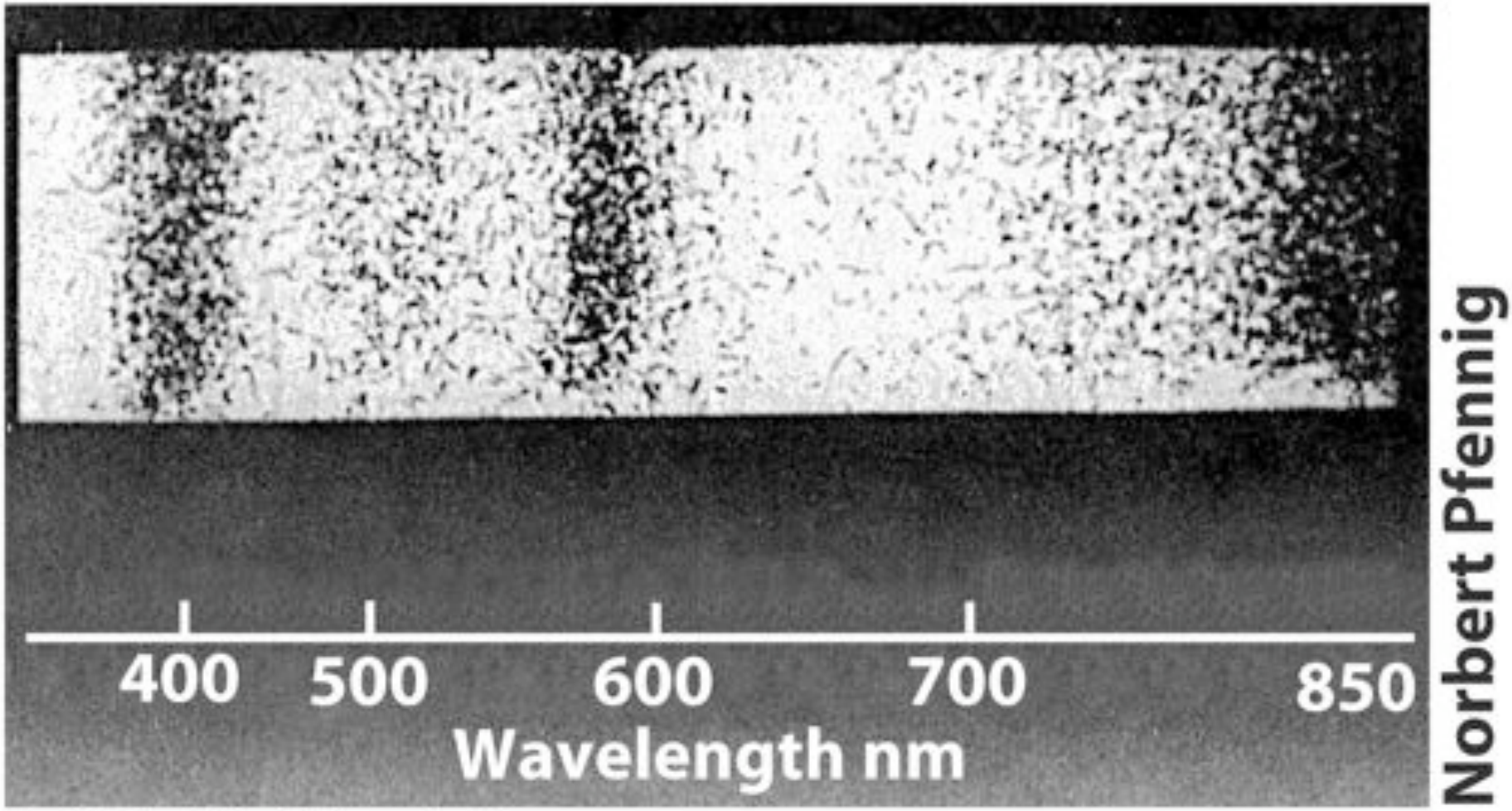

Figure 4-63a Brock Biology of Microorganisms 11/e

Bacterial waves

(chasing the gradient)

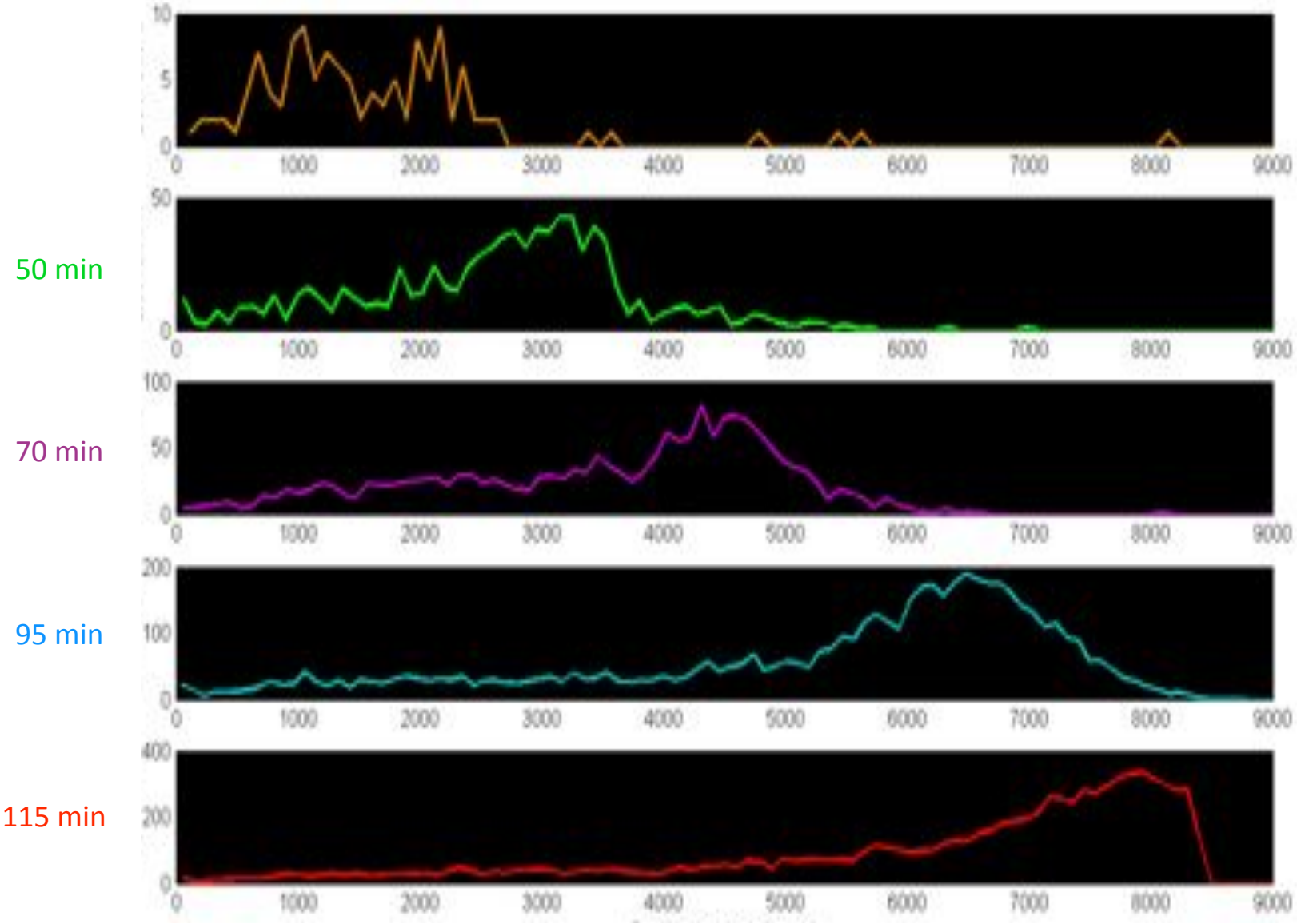

Ahmed & Stocker, unpublished

pH taxis

H. pylori: away from the stomach lumen, towards the epithelium

Do marine bacteria to this? (ocean acidification)

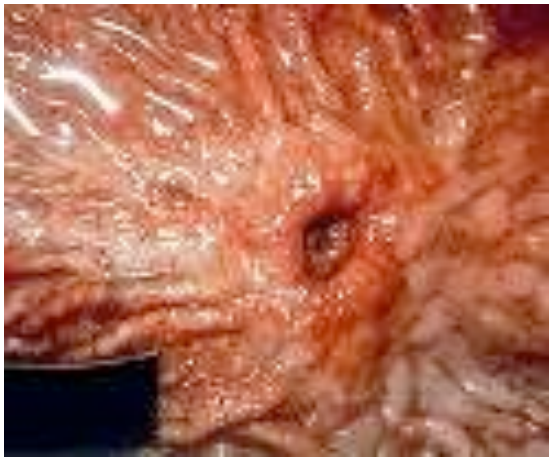

MAGNETOTAXIS

Magnetotaxis
[magnetite (Fe_3O_4) crystals]

agbac1/01.html

http://www.calpoly.edu/~rfrankel/magbac101.html

magnetosomes

≈ 1 μm

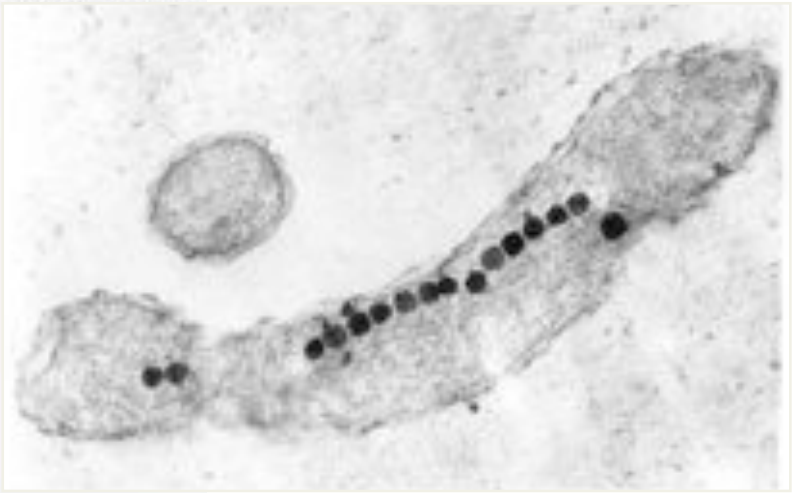

Figure 1 Transmission electron micrograph of Magnetospirillum magnetotacticum showing the chain of magnetosomes inside the cell. The magnetite crystals incorporated in the magnetosomes have cuboctaheral morphology and are ca. 42 nm long. The magnetosome chain is fixed in the cell and the interaction between the magnetic dipole moment associated with the chain and the local magnetic field causes the cell to be oriented along the magnetic field lines. Rotation of the cellular flagella (not shown) causes the cell to migrate along the field lines. Bar equals 1 micron.

- move preferentially North in N- hemisphere
  and South in S- "

↓

geomagnetic field inclined downwards
in both cases

→ 1-D random walk towards optimum O_2

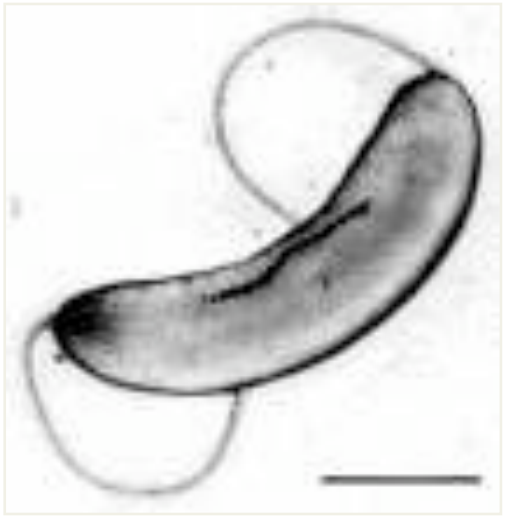

Recent insights on motility and chemotaxis in the Ocean

Vol. 25: 247–258, 2001 | AQUATIC MICROBIAL ECOLOGY
Aquat Microb Ecol | Published September 28

Bacterial motility in the sea and its ecological implications

Hans-Peter Grossart*, Lasse Riemann, Farooq Azam**

Scripps Institution of Oceanography, University of California San Diego, La Jolla, California 92093-0202, USA

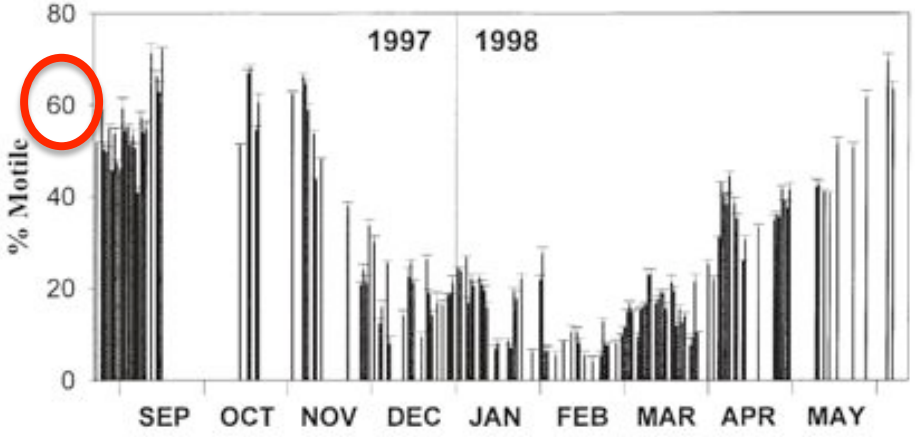

Fig. 1. Motility in natural bacterial assemblages (% motile) in surface waters off Scripps from August 1997 to June 1998. Samples were counted by dark-field microscopy (for details see 'Materials and methods')

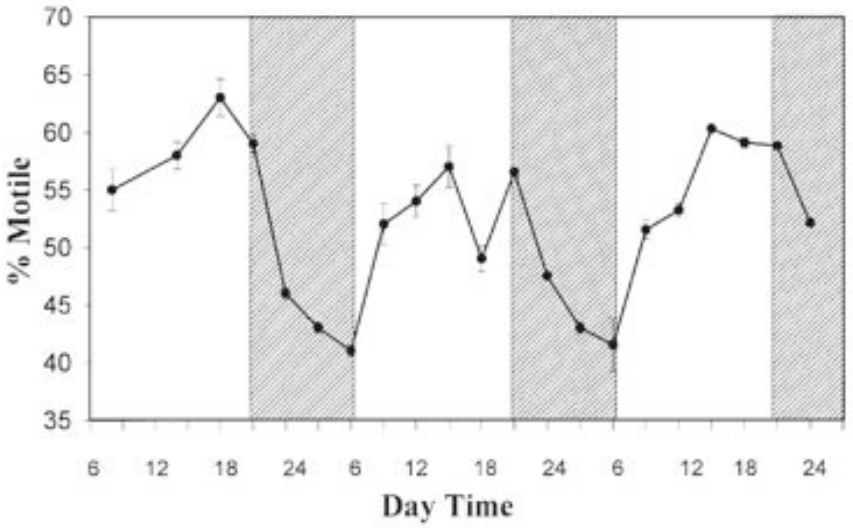

Fig. 2. Diel pattern of motility in natural bacterial assemblages (% motile) in surface waters off Scripps on 23 to 25 October 1997. Samples were counted by dark-field microscopy (for details see 'Materials and methods')

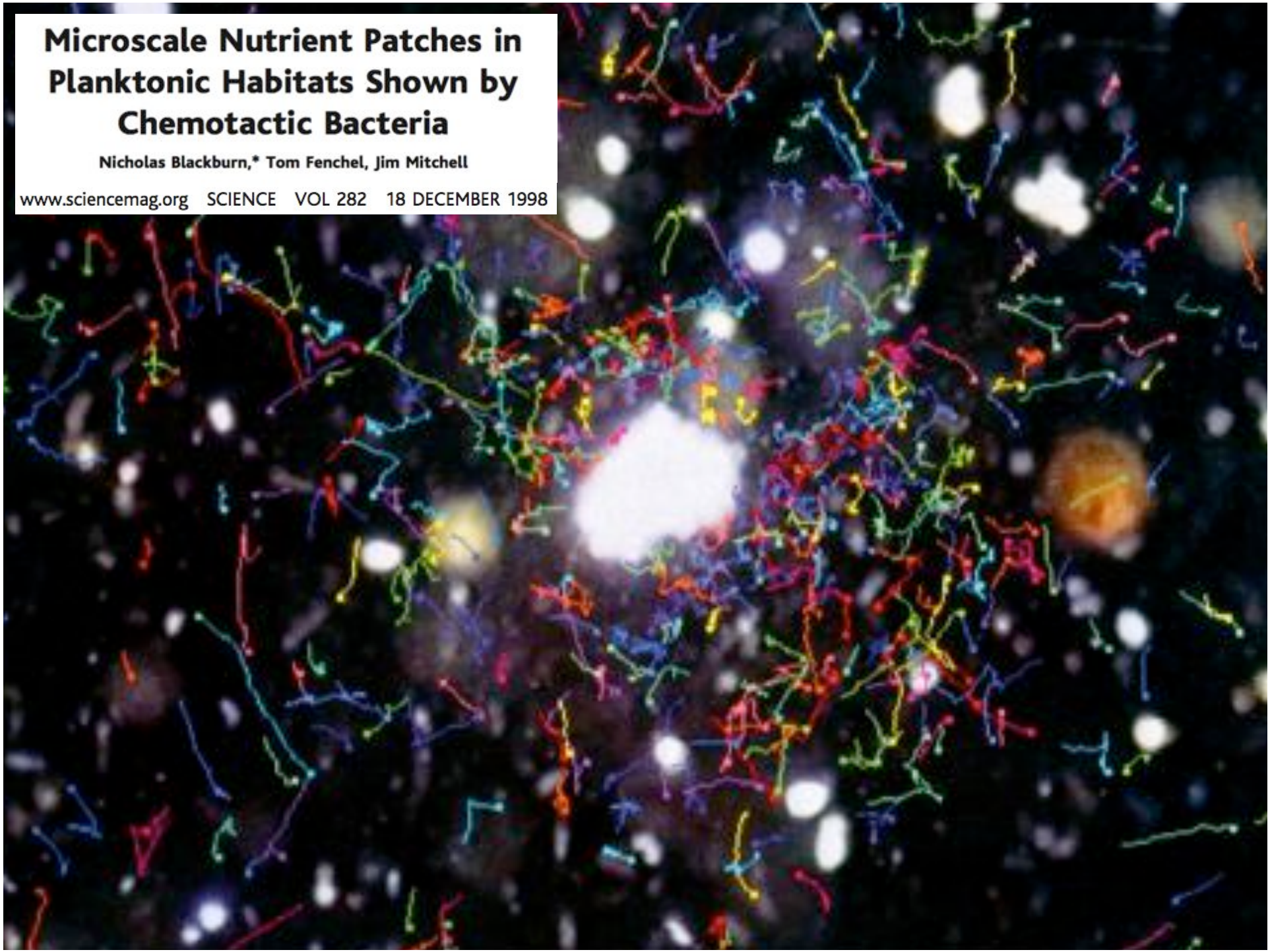

Microscale Nutrient Patches in Planktonic Habitats Shown by Chemotactic Bacteria

Nicholas Blackburn,* Tom Fenchel, Jim Mitchell

www.sciencemag.org SCIENCE VOL 282 18 DECEMBER 1998

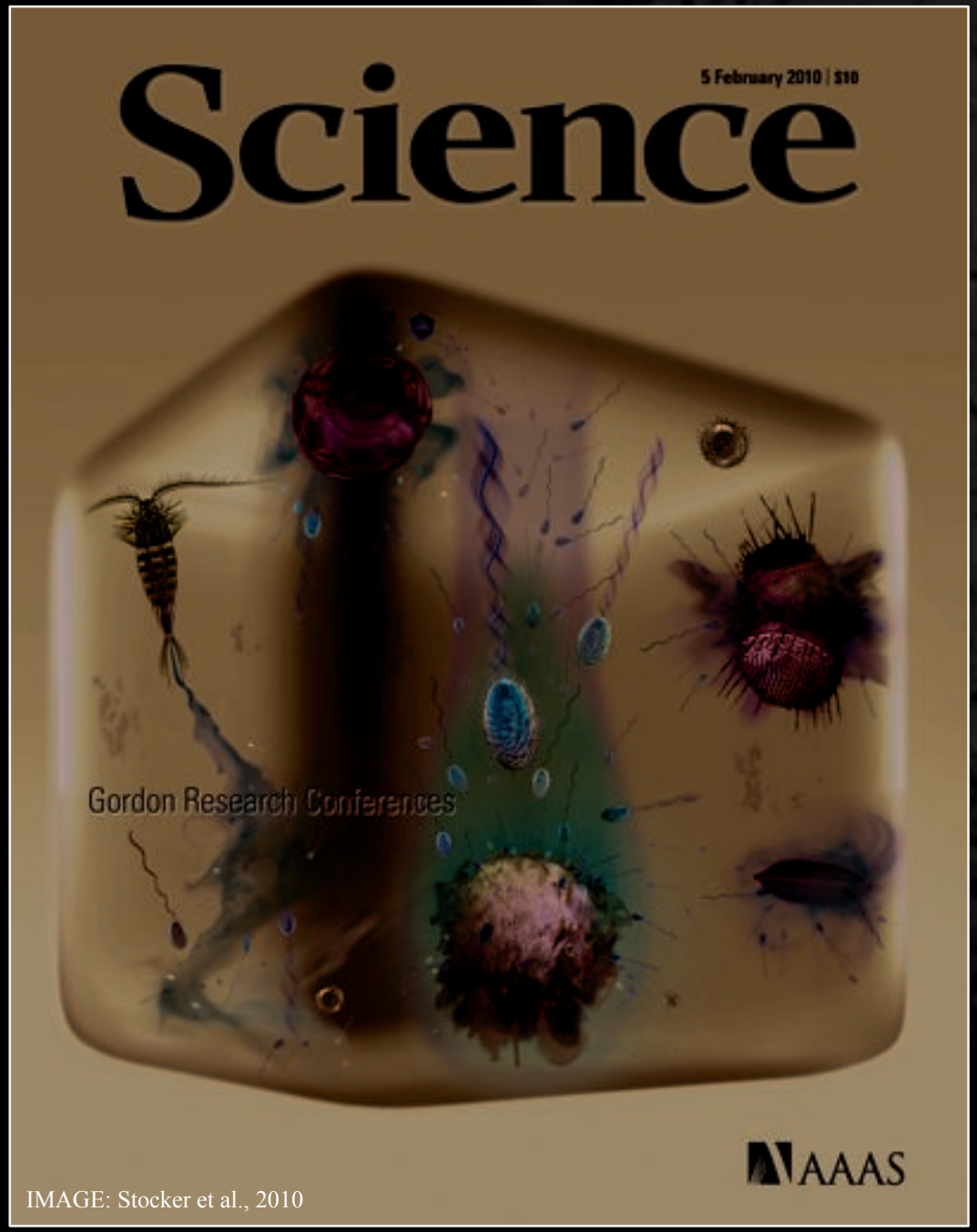

IMAGE: Stocker et al., 2010

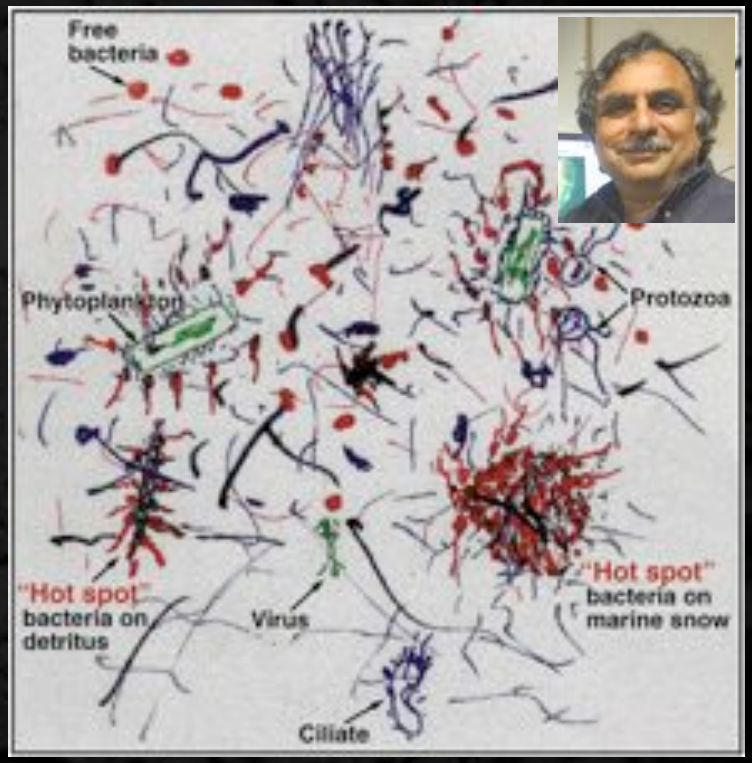

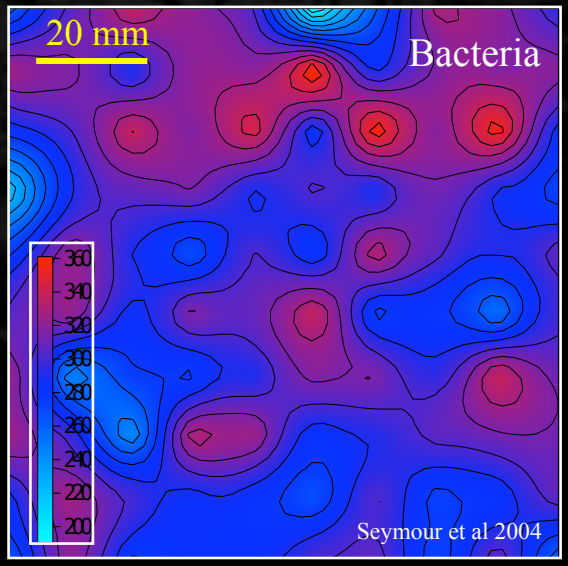

Long Lag Times and High Velocities in the Motility of Natural Assemblages of Marine Bacteria

JAMES G. MITCHELL,* LYNETTE PEARSON, ARMANDO BONAZINGA, SIMON DILLON, HELEN KHOURI, AND ROSEMARY PAXINOS

Biological Sciences, Flinders University, Adelaide, South Australia 5001, Australia

Received 22 September 1994/Accepted 14 December 1994

The motility characteristics of natural assemblages of coastal marine bacteria were examined. Initially, less than 10% of the bacteria were motile. A single addition of tryptic soy broth caused an increase in the motile fraction of cells but only after 7 to 12 h. Motility peaked at 15 to 30 h, when more than 80% of cells were motile. These results support the proposal that energy limits motility in the marine environment. Cell speeds changed more than an order of magnitude on timescales of milliseconds and hours. The maximum community speed was 144 μm s^{-1}, and the maximum individual burst velocity was 407 μm s^{-1}. In uniform medium, speed was

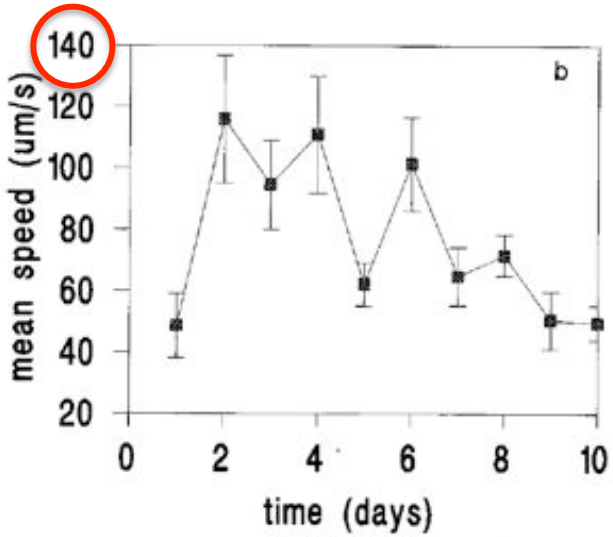

FIG. 2. Mean speed of motile cells as a function of time. (a) High-resolution sampling over a 50-h period. (b) Daily sampling over 9 days, with new bottles opened each day. Speed measurements were made in the center of the chamber away from surfaces. Zero values indicate that no motile cells were observed in these treatments. Sample sizes ranged between 10 and 25 cells for samples. Samples were assayed in triplicate. Error bars are 95% CI. Symbols in panel a show concentrations of TSB (wt/vol).

Rapid chemotaxis !

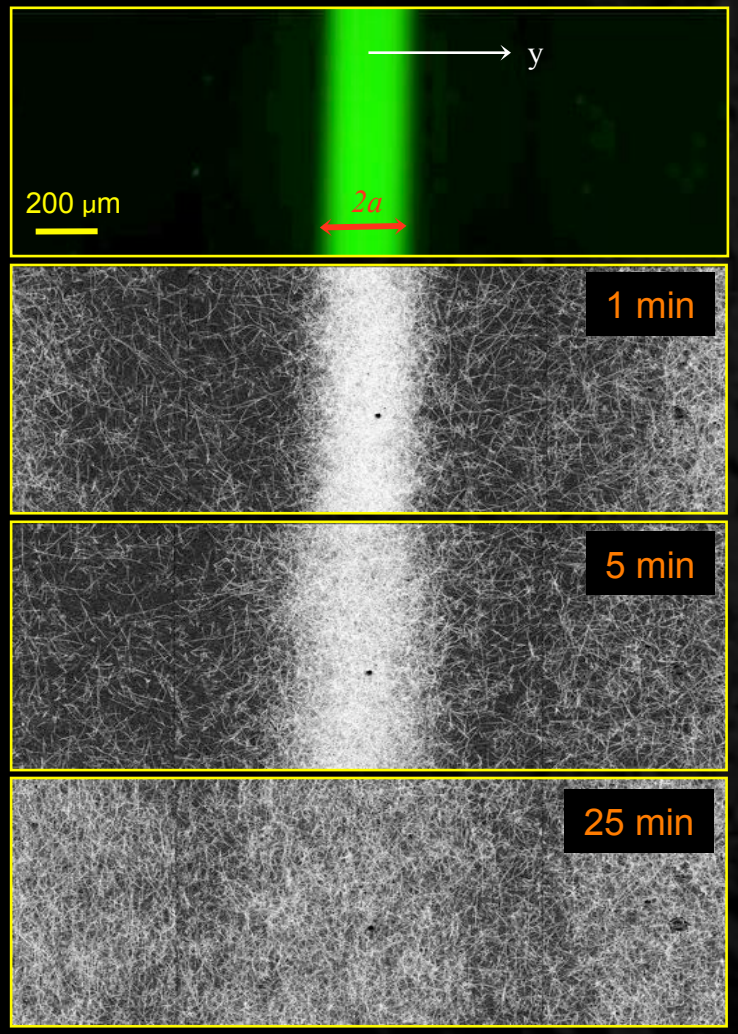

Pseudoalteromonas haloplanktis

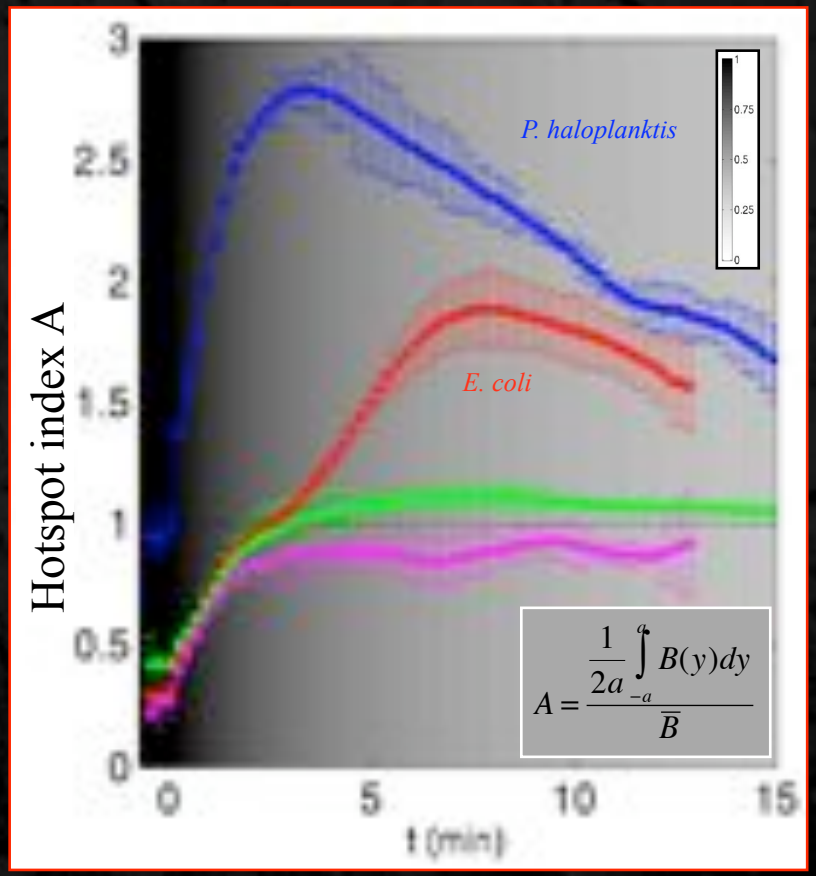

P. halo. control

E. coli control

$B(y)$ = bacterial distribution

- Rapid chemotaxis, 10-fold increase in nutrient gain
- Adaptation to aquatic nutrient landscape?

Stocker et al, PNAS 2008

FEMS Microbiology Ecology 44 (2003) 79–87

Bacterial tracking of motile algae

Greg M. Barbara *, James G. Mitchell

School of Biological Sciences, Flinders University of South Australia, G.P.O. Box 2100, Adelaide 5001, Australia

Received 24 May 2002; received in revised form 29 October 2002; accepted 8 November 2002

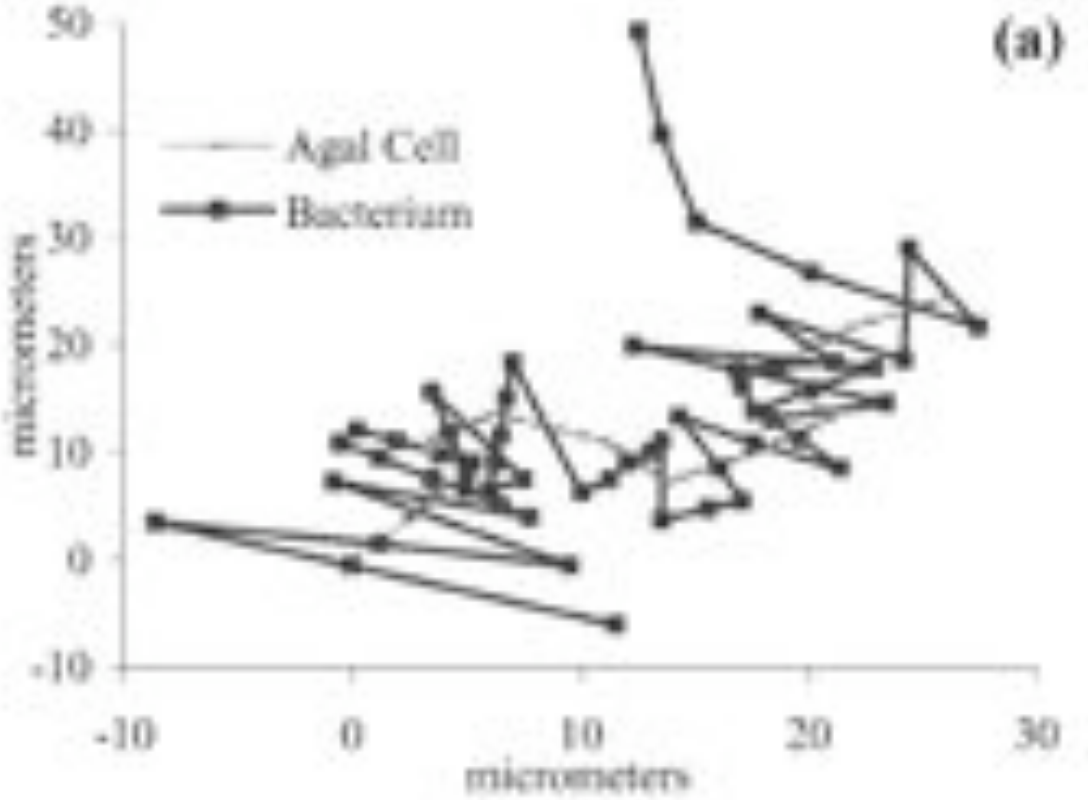

Super-effective chemotaxis?
Hydrodynamic effect? (Locsei & Pedley 2009)

Colonization of particle plumes

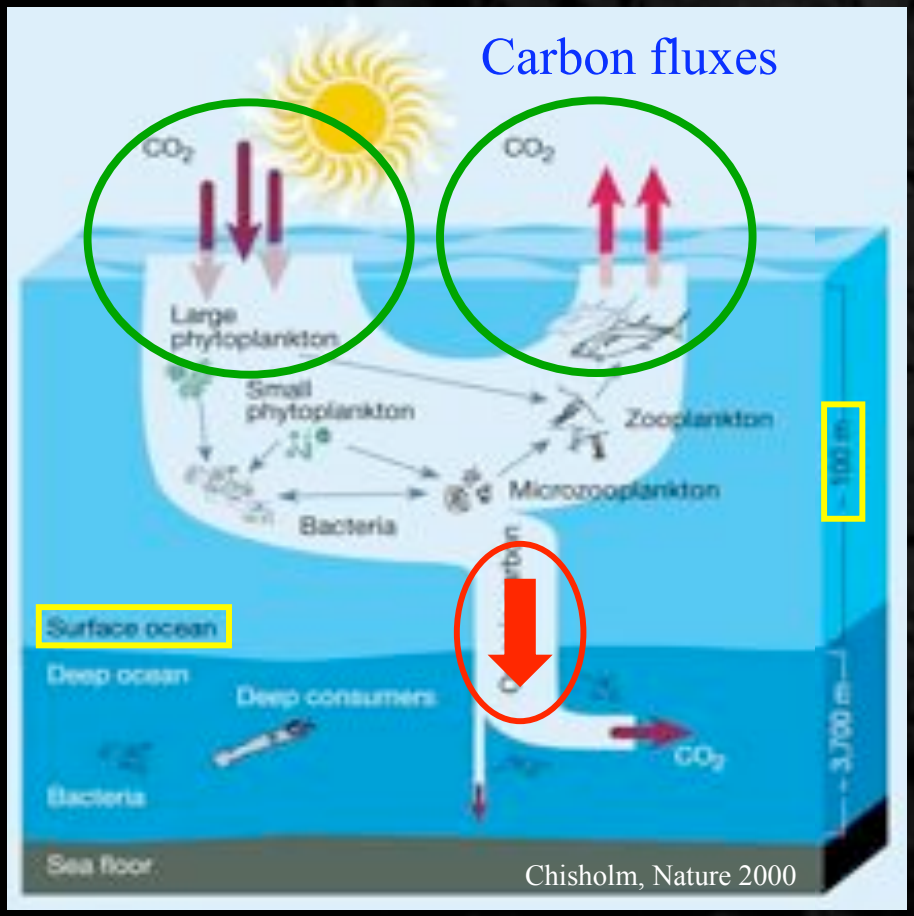

"The response of bacteria to sinking organic particles has a big influence on the oceanic carbon cycle" (Azam & Long Nature 2001)

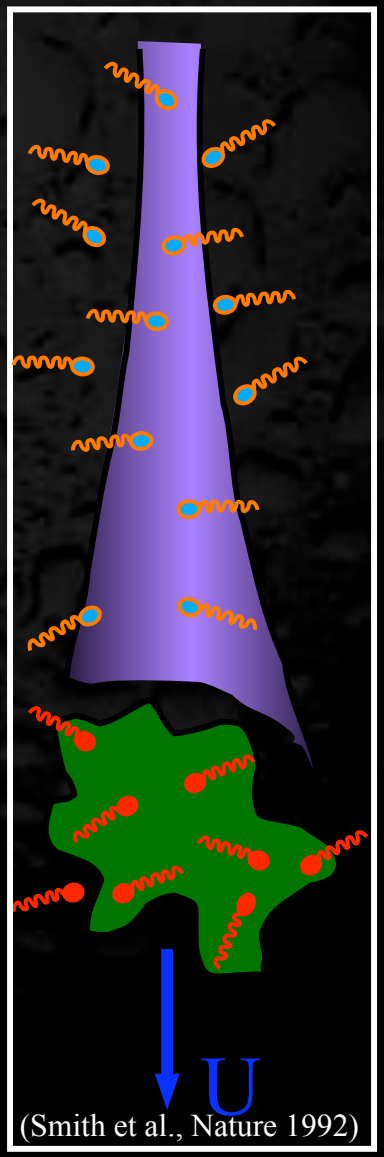

Plume: ecological niche for bacteria ?

Limnol. Oceanogr., 46(6), 2001, 1309–1318

Marine snow, organic solute plumes, and optimal chemosensory behavior of bacteria

Thomas Kiørboe
Danish Institute for Fisheries Research, Kavalergaarden 6, DK-2920 Charlottenlund, Denmark[1]

George A. Jackson
Department of Oceanography, Texas A&M University, College Station, Texas 77843

Abstract

Leaking organic solutes form an elongated plume in the wake of a sinking aggregate. These solutes may both be assimilated by suspended bacteria and guide bacteria with chemokinetic swimming behavior toward the aggregate. We used modifications of previously published models of the flow and concentration fields around sinking aggregates and of chemokinetic behavior of bacteria to identify the behavior that optimizes aggregate colonization and plume utilization. The optimal solution is governed by physical constraints and is a trade off between a high sensitivity to chemical signals and a long signal integration time. For a run-and-tumble swimming behavior, the predicted tumbling frequency is between 1 and 10 s^{-1}, similar to that reported for marine bacteria. The predicted optimal sensitivity to chemical signals is similar to or greater than that known for *Escherichia coli*. The optimal behavior was used to examine the potential contribution of aggregate-generated solute plumes for water column bacterial production. Despite occupying only a small volume fraction, the plumes may provide important growth habitats for free bacteria and account for a significant proportion of water column bacterial production at typical concentrations of marine snow aggregates.

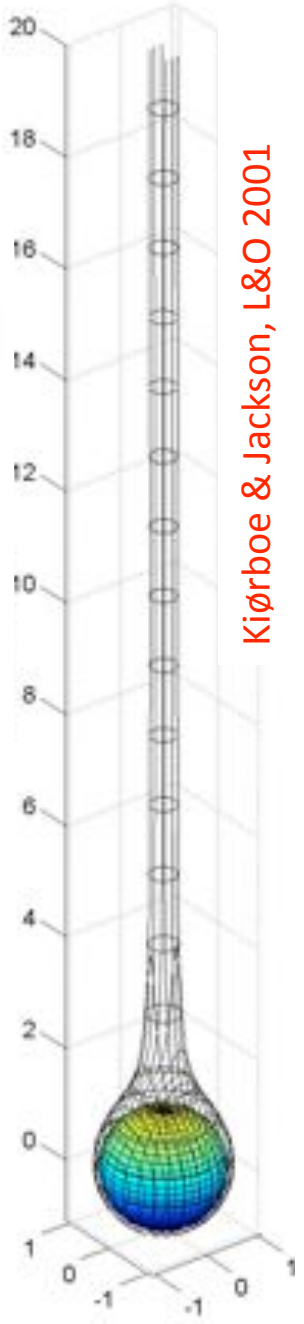

Kiørboe & Jackson, L&O 2001

Oceanography

Sea snow microcosms

Farooq Azam and Richard A. Long

Marine bacteria can respond to organic particles in sea water, creating hotspots of bacterial growth and carbon cycling. This microscale behaviour should be included in models of the oceanic carbon cycle.

NATURE | VOL 414 | 29 NOVEMBER 2001 | www.nature.com

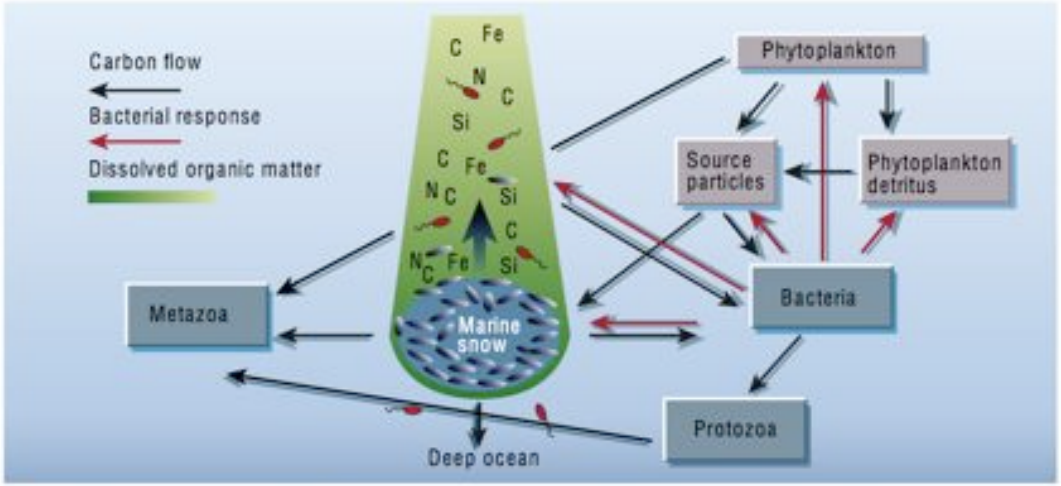

Figure 2 **Carbon fluxes in the ocean involving marine snow. The marine snow (aggregated phytoplankton and dead material) can sink into the deep ocean, thereby removing it from the upper ocean, or it can become involved in nutrient cycling. The first step is colonization by bacteria, which produce enzymes that turn the marine snow into dissolved organic matter (DOM). The colonizing bacteria produce DOM faster than they can use it, so the sinking snow releases a plume of material containing carbon (C), nitrogen (N), silicon (Si) and iron (Fe). Other free-living bacteria (red) are attracted to the plume and grow rapidly. Colonizers may also release their progeny (blue) into the plume. High concentrations of bacteria attract protozoa, which in turn attract larger animals (metazoa). The marine snow and the plume may thus become the focus of a complex food web.**

Rapid chemotactic response enables marine bacteria to exploit ephemeral microscale nutrient patches

Roman Stocker*†, Justin R. Seymour*, Azadeh Samadani‡, Dana E. Hunt*, and Martin F. Polz*

*Department of Civil and Environmental Engineering, Massachusetts Institute of Technology, 77 Massachusetts Avenue, Cambridge, MA 02139; and ‡Department of Physics, Brandeis University, 415 South Street, Waltham, MA 02454

Edited by David M. Karl, University of Hawaii, Honolulu, HI, and approved January 22, 2008 (received for review October 14, 2007)

PNAS | March 18, 2008 | vol. 105 | no. 11 | 4209–4214

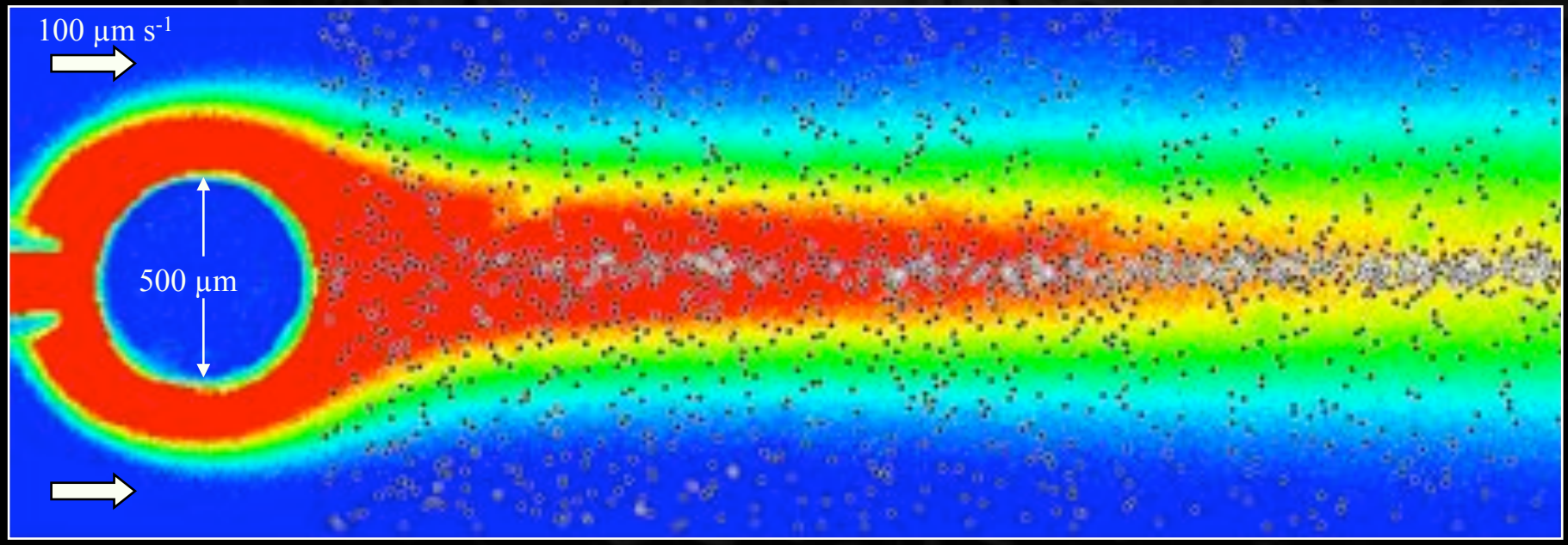

Accumulation in the plume

Microfluidics

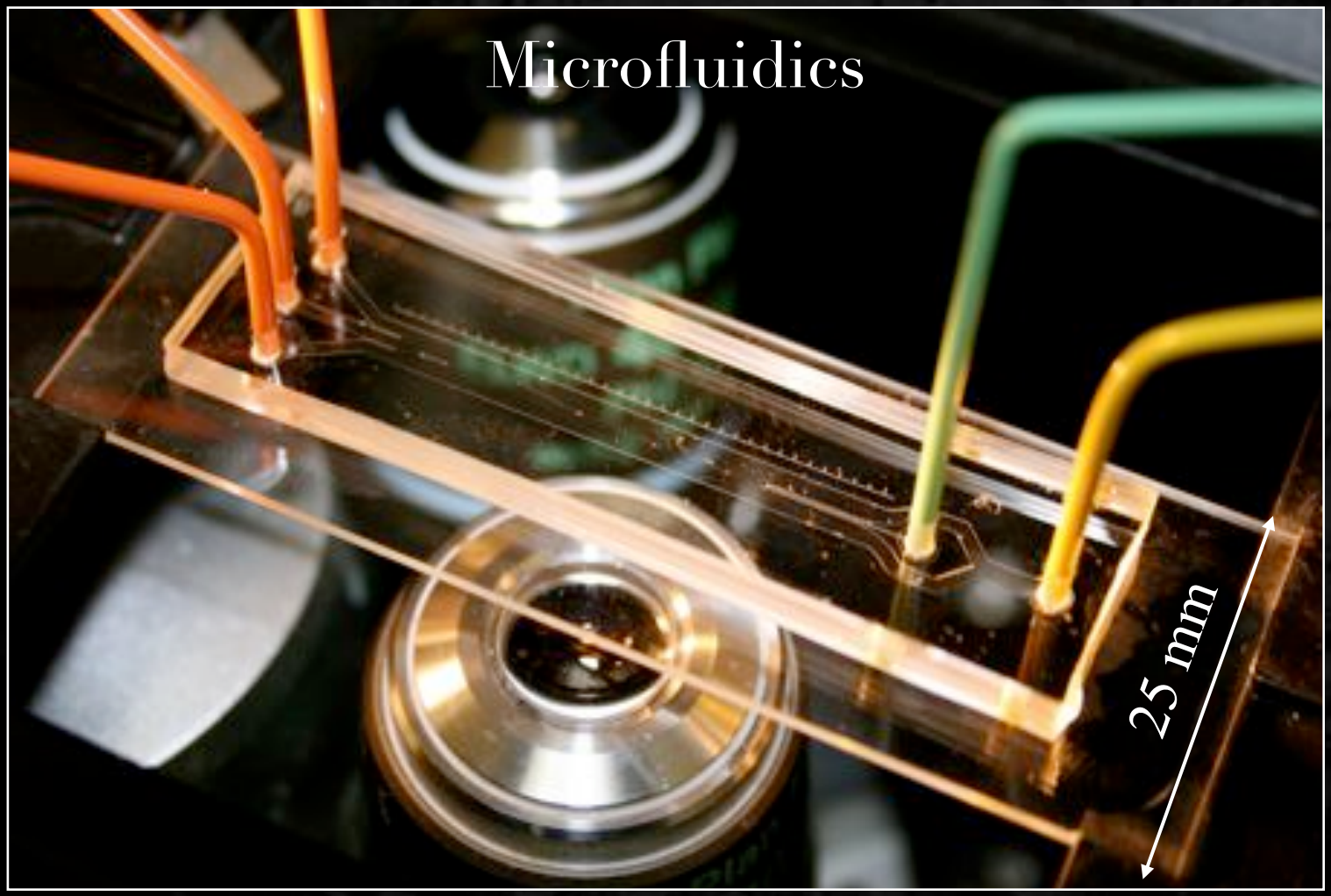

Ideal for studying microbial processes:

- Low Reynolds number: the flow regime of microbes
- Accuracy: geometry (~5 μm), flows (μm/s), chemical gradients (low Re)
- Transparent: track single bacteria
- Versatile experimental platform

Stocker et al, PNAS 2008; **Seymour et al, L&O Methods 2008;**
Am Nat 2009; JoVE 2008; JPR 2009; AME 2010; Science, in press

Microfabrication

Soft lithography (Whitesides *et al* 2001)

- Design channels (CAD)
- Print mask (transparency)
- Spin-coat photoresist on wafer
  (thickness = channel depth)
- Align mask and expose to UV
- Develop wafer
  (wash off unlinked photoresist)

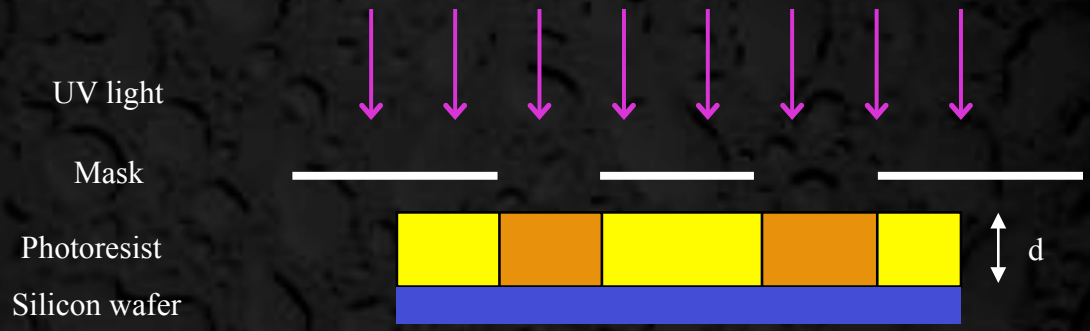

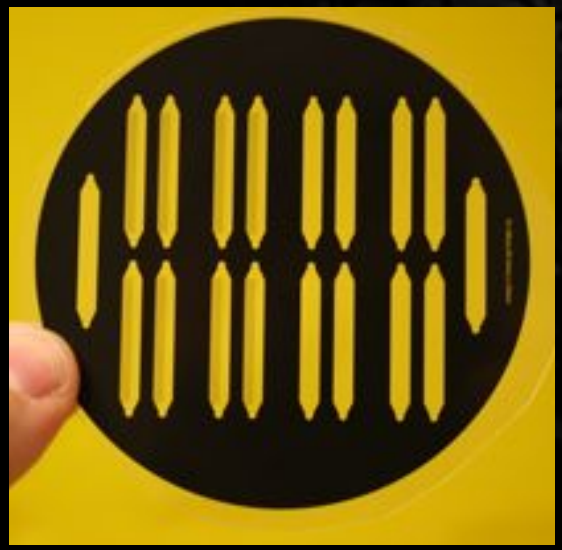

Mask (transparency)

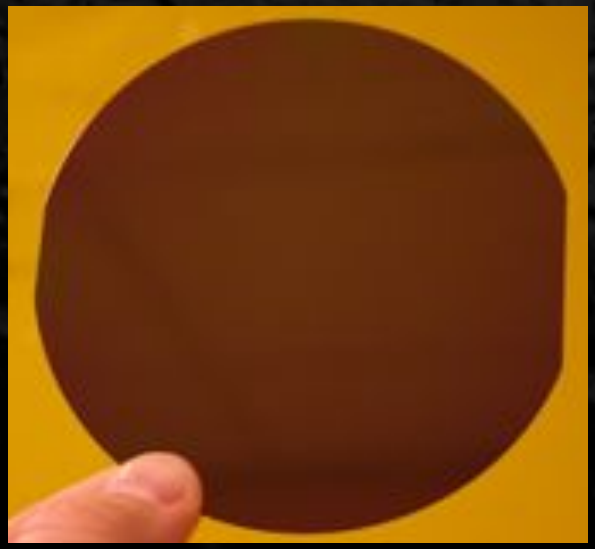

Silicon wafer

Developed wafer

Microfabrication

- Cast PDMS and cure in oven
- Peel PDMS off wafer
- Make holes (inlets and outlets)
- Bond to glass slide (oxidized)
- Connect tubing and syringe
- Videomicroscopy

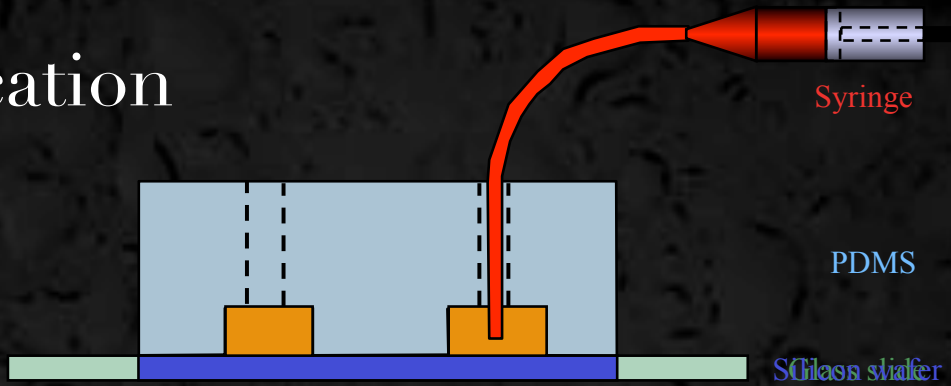

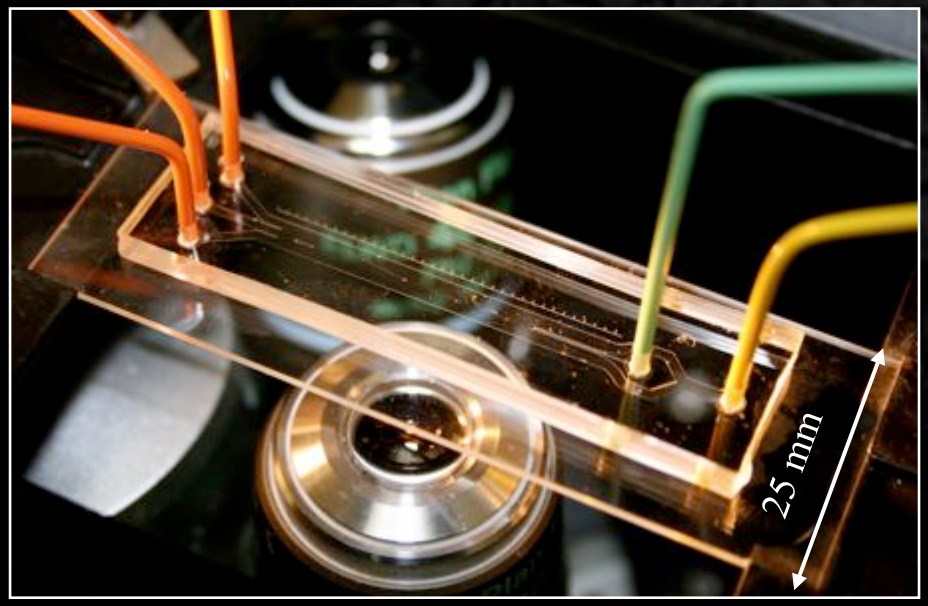

Phase-contrast inverted microscope

Visualization

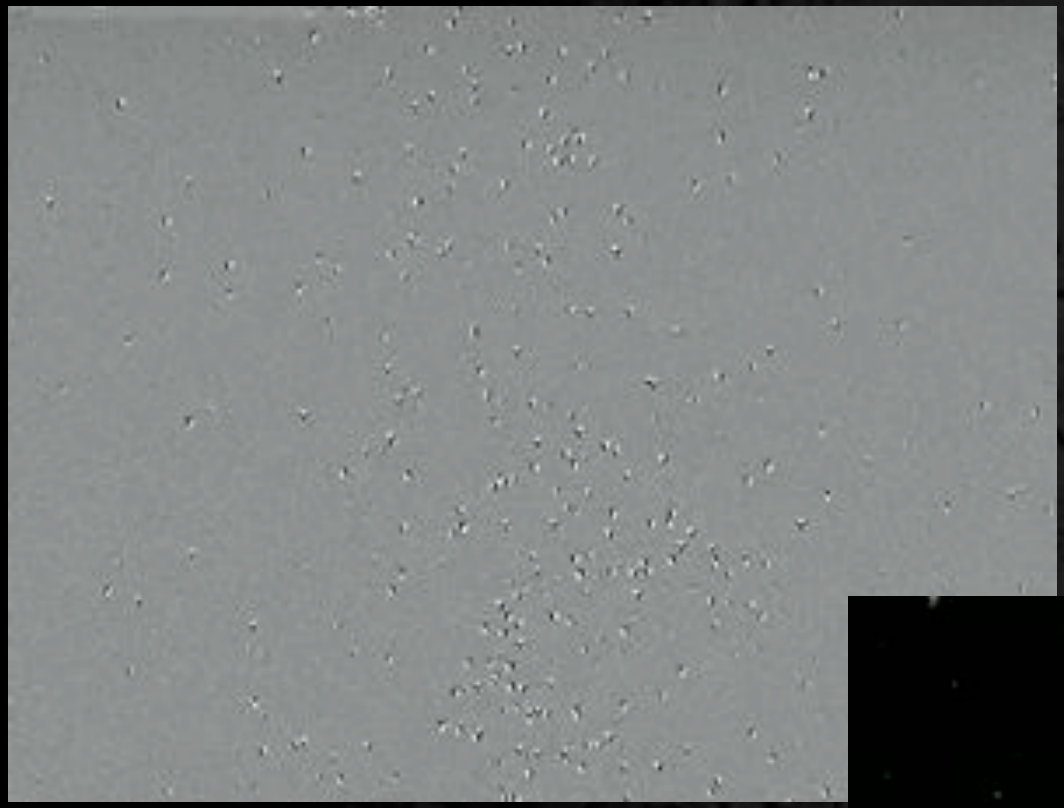

Foraging in turbulent waters

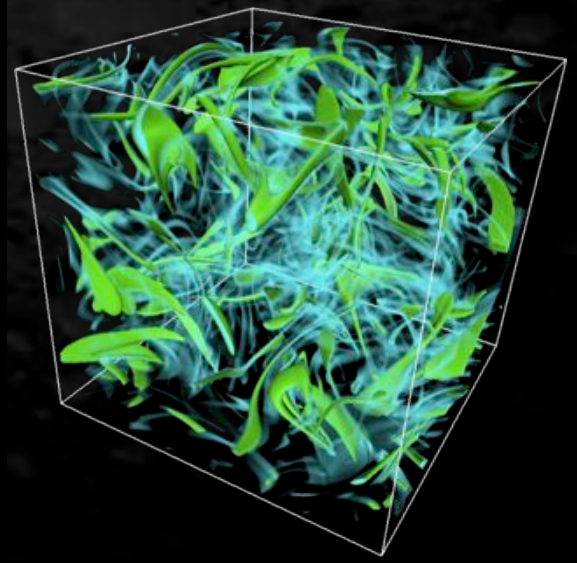

Taylor & Stocker, in prep.